www.MaterialsViews.com

Production of Two-Dimensional Nanomaterials via Liquid-Based Direct Exfoliation

*Liyong Niu, Jonathan N. Coleman, Hua Zhang, Hyeonsuk Shin, Manish Chhowalla, and Zijian Zheng**

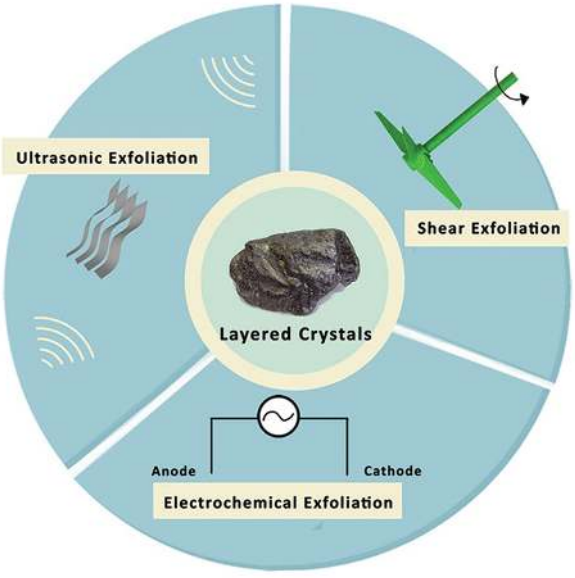

Liquid-Based Direct Exfoliation

From the Contents

Tremendous efforts have been devoted to the synthesis and application of two-dimensional (2D) nanomaterials due to their extraordinary and unique properties in electronics, photonics, catalysis, etc., upon exfoliation from their bulk counterparts. One of the greatest challenges that scientists are confronted with is how to produce large quantities of 2D nanomaterials of high quality in a commercially viable way. This review summarizes the state-of-the-art of the production of 2D nanomaterials using liquid-based direct exfoliation (LBE), a very promising and highly scalable wet approach for synthesizing high quality 2D nanomaterials in mild conditions. LBE is a collection of methods that directly exfoliates bulk layered materials into thin flakes of 2D nanomaterials in liquid media without any, or with a minimum degree of, chemical reactions, so as to maintain the high crystallinity of 2D nanomaterials. Different synthetic methods are categorized in the following, in which material characteristics including dispersion concentration, flake thickness, flake size and some applications are discussed in detail. At the end, we provide an overview of the advantages and disadvantages of such synthetic methods of LBE and propose future perspectives.

small NANO MICRO

1. Introduction

In the wake of graphene's discovery, layered two-dimensional (2D) nanomaterials have regained intensive research attention due to their distinctive and unique properties. To date, plenty of layered 2D nanomaterials have been reported, which can be categorized into groups based on their structural similarities as follows.[1] One group features hexagonal nanosheets with atomic thickness, such as graphene and boron nitride (h-BN). Another group contains transition metal dichalcogenides (TMDs) (e.g., MoS_2 and $MoSe_2$) and metal halides (e.g., PbI_2 and $MgBr_2$).[2] They exhibit near-identical structures, in which a metal layer is sandwiched between two adjacent chalcogen/halide layers. The third group is layered metal oxides (e.g., MnO_2 and MoO_3) and layered double hydroxides such as $Mg_6Al_2(OH)_{16}$.[3] Moreover, an emerging, large family of 2D early transition metal carbides or carbonitrides, labeled as MXenes was discovered.[4] Scientists have extensively reported the diverse properties and a wide range of applications upon the exfoliation of bulk-layered materials into these single- or few-layered 2D nanosheets.[5–9] The most studied 2D nanomaterial, graphene, can be considered as an example. Single layered graphene possesses high intrinsic mobility (2×10^5 cm^2 V^{-1} s^{-1}), large theoretical surface area (2630 m^2 g^{-1}), high thermal conductivity (≈5000 W m^{-1} K^{-1}) and Young's modulus (≈1.0 TPa), high optical absorption (>2%) and good electrical conductivity.[10–13] Such unique and outstanding properties have been demonstrated to be important for a wide range of applications. Graphene has been used in flexible electronics, such as touch screen displays, electronic papers and organic light emitting diodes, which require low sheet resistance and high transmittance. Its excellent mechanical stability and chemical durability make it superior to rigid and expensive indium tin oxide (ITO). Furthermore, it could be fabricated into field effect transistors (FET) with logic functions[14] or high frequency[15] by opening the bandgap of graphene via nanostructuring[16,17] or chemical functionalization.[18] In photonics, graphene is applicable for photodetectors[19] and optical modulators[20] due to its broad absorption ranging from ultraviolet to infrared and ultrafast response. In addition, graphene has become a promising candidate in the search for new materials to build highly efficient and renewable energy generation and storage devices, such as lithium-ion (Li-ion) batteries, organic solar cells, dye-sensitized solar cells, and supercapacitors, amongst others. Excellent performances for 2D nanomaterials other than graphene are also coming to light. Some of these are being intensively investigated in terms of their properties and applications, such as h-BN and TMDs,[21–23] while others have only recently been reported, such as 2D double hydroxides and MXene. Regarding h-BN, its wide direct band gap of 5.8 eV, high thermal conductivity (≈390 W m^{-1} K^{-1})[24] and strong oxidation resistance (stable at 1500 °C in air)[25] not only enables its use as a dielectric layer in electronic devices but other device applications requiring efficient heat dissipation and oxidation resistance can also be met.

Despite the extensive research in materials' characteristics and applications, scientists and engineers also face another tremendously challenging question: how can a large quantity of these 2D nanomaterials be produced with high quality in a commercially viable way? This is of paramount importance for industry to decide if these new materials will ultimately be used for large scale applications. Up until now, quite a few different methods have been developed for the production of layered 2D nanomaterials, including bottom-up synthesis by chemical vapor deposition (CVD) and epitaxial growth, and top-down exfoliation approaches by micromechanical cleavage, chemical exfoliation and liquid-based ultrasonic exfoliation. Bottom-up CVD synthesis is regarded as an important method to synthesize 2D nanomaterials, in which precursors react on transition metal substrates at high temperature to form single- or few-layered 2D nanosheets. This method can produce graphene and some other TMDs with high quality; however, it requires harsh growth conditions such as high temperature and high vacuum, and is size-limited. The additional transfer process from the metal surface to target substrates further introduces residues and defects that will deteriorate their performance. Intensive research efforts are being undertaken to improve CVD synthesis and transfer processes, and a great progress has been made. Those works are however outwith the scope of this review.

On the other hand, because layered materials comprise strong in-plane chemical bonds but a weak out-of-plane interaction, namely van der Waals force, complete top-down exfoliation of these bulk layered materials to yield thin nanosheets at nanometer or even atomic thickness is possible.

L. Y. Niu, Prof. Z. J. Zheng
Nanotechnology Center
Institute of Textiles and Clothing
The Hong Kong Polytechnic University, Hung Hom
Kowloon, Hong Kong SAR, China
E-mail: tczzheng@polyu.edu.hk

L. Y. Niu, Prof. Z. J. Zheng
Advanced Research Center for Fashion and Textiles
The Hong Kong Polytechnic University
Shenzhen Research Institute
Shenzhen 518000, China

Prof. J. N. Coleman
School of Physics
CRANN and AMBER
Trinity College Dublin
Dublin 2, Ireland

Prof. H. Zhang
Center for Programmable Materials
School of Materials Science and Engineering
Nanyang Technological University
50 Nanyang Avenue, Singapore 639798, Singapore

Prof. H. S. Shin
Department of Chemistry and Department of Energy Engineering
Ulsan National Institute of Science and Technology
Ulsan 689–798, Republic of Korea

Prof. M. Chhowalla
Materials Science and Engineering
Rutgers University
607 Taylor Road, Piscataway, NJ 08854, USA

DOI: 10.1002/smll.201502207

Micromechanical cleavage, although demonstrating the possibility of this idea, can only produce samples for fundamental study because of its extremely low throughput. Chemical exfoliation, which particularly refers to the synthesis of graphene oxide (GO) via chemical oxidation of graphite to form graphite oxide and subsequent ultrasonic exfoliation, is low-cost and highly scalable. Nevertheless, the oxygen-containing defects of GO cannot be fully eliminated even after chemical or thermal reduction, which significantly limits the applications in electronic and optical devices.[12,26,27]

More recently, a new top-down exfoliation strategy, namely liquid-based direct exfoliation (LBE), shows remarkable progress in making many kinds of 2D nanomaterials. LBE refers to a collection of methods that directly exfoliate bulk layered materials into 2D nanomaterials in the liquid media without the need for chemical oxidation of the bulk materials (**Scheme 1**). It includes not only ultrasonic exfoliation in organic solvents, but also other approaches where the exfoliation process mainly occurs by taking advantage of the liquid media, such as the liquid phase exfoliation by surfactants, ionic liquids, salts, the electrochemical exfoliation in various liquid media, and the shear exfoliation method. This LBE strategy is gaining more and more attention because it represents an extraordinarily versatile, potentially up-scalable and sustainable route for the production of a wide variety of (or virtually any) 2D nanomaterials. The 2D nanomaterials present desirable material properties and good solution dispersing ability, which significantly facilitates the formation of functional composites and hybrids by simple mixing, and is also convenient for casting onto different thin films for device and coating applications.

In view of these great advantage and the rapid progress that is being made, this article aims to provide a comprehensive and up-to-date review on the synthesis of 2D nanomaterials including graphene, TMDs, newly emerging phosphorene and MXene, and other materials using LBE strategies (**Table 1**). The sections of thisreview are categorized according to different LBE methods. Although some applications are mentioned briefly in our review, we intend to focus mainly on synthesis methods and and materials characteristics. For 2D nanomaterials produced by other synthetic methods and their applications, readers may refer to some other published reviews.[1,23,28–32]

Liyong Niu received his BS in materials chemistry at Henan University in 2009. He is currently a PhD candidate at the Nanotechnology Center of the Institute of Textiles and Clothing at Hong Kong Polytechnic University. His work in Prof. Z. Zheng's group includes the synthesis and application of 2D nanomaterials.

Jonathan Coleman Jonathan Coleman is the Professor of Chemical Physics at Trinity College Dublin and a Principle Investigator at the CRANN nanoscience centre. His group works on solution-processed thin films for transparent conducting applications and high-strength nanostructured composites. **Hua Zhang** is a Professor at Nanyang Technological University. He focuses on the synthesis of 2D nanomaterials, graphene and carbon nanotubes, and their hybrid composites for application in sensors, clean energy, and water remediation. **Hyeon Suk Shin** is an Associate Professor at UNIST, Korea. His research focuses on 2D materials, including graphene, h-BN, transition-metal dichalcogenides, their heterostructures, and their applications for electrocatalysts and (opto)electronic devices. **Manish Chhowalla** is currently a Professor and Associate Chair at Rutgers University. He is interested in understanding the role of disorder in determining material properties as well as phase engineering in low-dimensional materials.

Zijian Zheng is currently an Associate Professor of the Institute of Textiles and Clothing at the Hong Kong Polytechnic University. He received his BEng in Polymer Materials and Engineering at Tsinghua University (2003) and his PhD in Chemistry at the University of Cambridge (2007). His research interests include the development of surface-patterning techniques, the synthesis and application of 2D nanomaterials, structuring polymer architectures, and wearable energy-storage devices.

2. Direct Ultrasonic Exfoliation in Liquid

Direct ultrasonic exfoliation in liquid is a major component of LBE. It refers to a collection of methods, which produce 2D nanosheets by direct ultrasonication of their bulk materials in liquid media. There are two crucial parameters involved in this method. One is the commonly required ultrasonication (bath sonication or probe sonication). Layered materials can be successfully exfoliated upon exposure to the ultrasonic waves. Such waves can generate shear forces or cavitation bubbles,[150] which will provide high energy upon collapse of bubbles or voids in liquids to break up the layered structure and produce single- or few-layered nanosheets. The liquid media, such as the organic solvent or the aqueous solutions of stabilizers, ionic liquids, and salts, also plays an important role in the reduction of the potential energy barrier that exists in the interlayers of the bulk materials, and in the subsequent stabilization of nanosheets via interfacial interactions. Based on the liquid media used, this part of the review is divided into several sections to discuss the exfoliation process, the quality of the products, and some applications in detail.

2.1. Organic Solvent-Based Exfoliation

This method involves the dispersion of bulk layered materials in a selected organic solvent, ultrasonic exfoliation and subsequent purification process. It is known that the interfacial tension between solid and liquid media plays an important role in their interactions. A suitable solvent will reduce the potential energy between adjacent layers (energy minimization) to

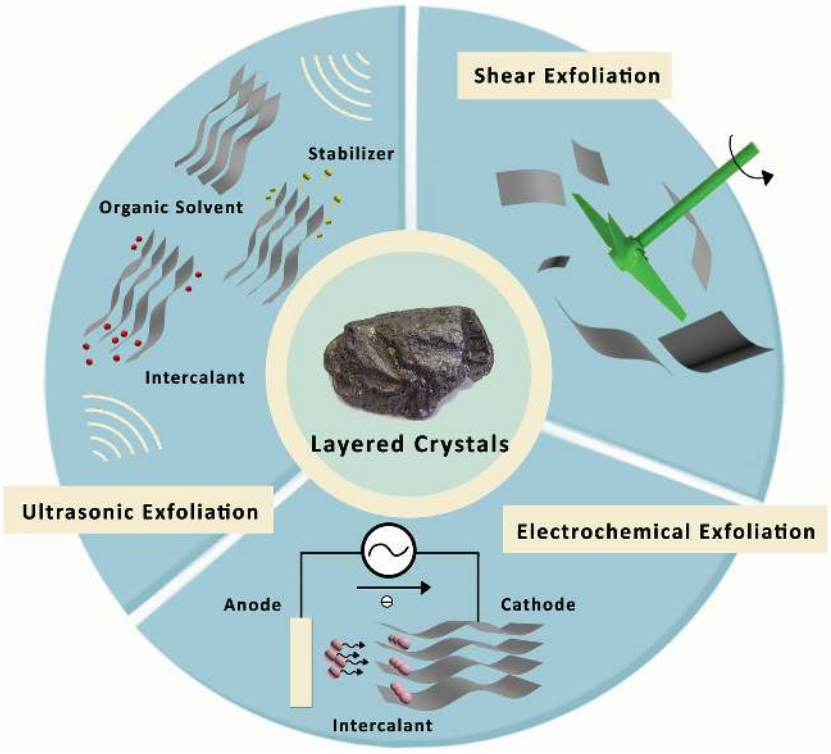

Scheme 1. Production of 2D nanomaterials via liquid-based direct exfoliation of bulk layered crystals.

overcome the van der Waals attraction and the solvent–nanosheets interaction could balance the inter-sheet attractive forces to stabilize the dispersion of nanosheets.[151] Two independent groups reported the first successful direct exfoliation of natural graphite powders in organic solvents in 2008.[152,33] Many efforts have since been devoted to a more in-depth study of the interaction between organic solvents and solid flakes, pursuit of proper solvents for effective exfoliation, and improvement of the stability of concentrated dispersion of graphene sheets.

2.1.1. Exfoliation in Good Solvents

Coleman's group performed a library survey of organic solvents used in the liquid exfoliation of graphite. They found that the best solvents for producing large quantities of graphene sheets should have a surface tension around 40 mJ m^{-2} (equal to a surface energy of 70 mJ m^{-2}), such as *N*-methyl-2-pyrrolidone (NMP ≈40 mJ m^{-2}), and *N,N*-dimethylformamide (DMF ≈37.1 mJ m^{-2}), which matches the surface energy of graphene (68 mJ m^{-2}, **Figure 1**a). A more useful parameter was further deduced, i.e., the Hansen solubility parameter, which is the square root of dispersive, polar and hydrogen bonding components of the cohesive energy density of a material.[33] This much more precise parameter allows one to search for new solvents. The absence of the D band of large graphene flakes in Raman measurements confirmed the ultrasonic process (30 min) did not introduce any structural defects, while its appearance in small graphene flakes was mainly due to the edge defects (Figure 1b). As characterized by transmission electron microscopy (TEM) (Figure 1c, d), the exfoliated graphene sheets are single- or few-layered (≈1 wt% monolayer), with a dispersion concentration of ≈0.01 mg mL^{-1} and a size ranging from ≈500 nm to ≈3 μm.

However, such a concentration is too low to meet the practical demands of large quantities, so some approaches

Table 1. Summary of 2D nanomaterials produced by LBE strategy.

LBE			2D nanomaterials	Reference
Direct ultrasonic exfoliation in liquid	Organic solvent-based exfoliation	Good solvents	Graphene, TMDs, h-BN, phosphorene	[33–59]
		Low boiling point solvents		
	Stabilizer-based exfoliation	Ionic surfactants	Graphene, TMDs, h-$BNMnO_2$	[60–68]
		Non-ionic surfactants		[69–71]
		Polymers		[72–76]
		Pyrene derivatives		[77–84]
	IL-based exfoliation		Graphene	[85,86]
	Salt-assisted exfoliation		Graphene, TMDs	[87,88]
	Intercalant-assisted exfoliation	Li^+	Graphene, TMDs, h-BN, MXene	[89–96]
		Acids		[97,98]
		Organic molecules		[4,99–110]
	Ion exchange-based exfoliation		Metal oxide, LDH	[111–115]
Electrochemical exfoliation	Anionic intercalations		Graphene, TMDs, h-BN	[116–120,127,128]
	Cationic intercalations			[129–143]
Shear exfoliation			Graphene, TMDs, h-BN	[144–149]

have been attempted to improve graphene yield, such as selecting alternative organic solvents. Hamilton et al. chose a nonpolar solvent, ortho-dichlorobenzene (ODCB), to produce homogenous dispersions of graphene nanosheets. With a surface tension of 36.6 mJ m^{-2},[it] can interact with graphene via π–π stacking and is compatible with a variety of reaction chemistries.[34] However, the concentration was only increased to 0.03 mg mL^{-1}. Bourlinos and co-workers, who proposed a peculiar class of perfluorinated aromatic molecules, including hexafluorobenzene (C_6F_6), octafluorotoluene ($C_6F_5CF_3$), pentafluorobenzonitrile (C_6F_5CN) and pentafluoropyridine (C_5F_5N), expanded the choices of suitable organic solvents to solubilize graphene.[35] Beyond the surface energy matching between solvent and graphene, they claimed that donor–acceptor interactions might be another driving force for the exfoliation. The presence of strong electron-drawing fluorine atoms would involve charge transfer via π–π stacking. Among those solvents, C_6F_5CN leads to the highest concentration of graphene sheets (≈0.1 mg mL^{-1}) with thickness of 0.5–2 nm. The rest exhibited a less powerful dispersive ability with decreasing order: C_6F_5CN > C_6F_6 > C_5F_5N > $C_6F_5CF_3$. As controls, analogous hydrocarbon solvents such as benzene, toluene, nitrobenzene and pyridine failed to give stable and high concentrations.

Apart from searching for more suitable solvents, other factors such as ultrasonication time and power are also investigated to increase the yield. Khan et al. reported improved graphene concentrations up to 1.2 mg mL^{-1} with ≈4 wt% monolayers by simple low-power ultrasonication in NMP for very long time, up to 460 h.[36] **Figure 2**a shows the concentration of graphene as a function of sonication time. Longer sonication times lead to higher concentrations, nevertheless, the flake dimensions decreased accordingly, by the reverse of square root of time ($t^{-1/2}$). The mean flake length still remained around 1 μm (Figure 2b). Defects were also induced by long sonication times, which were predominately attributed to edge defects rather than basal plane. Later Khan and co-workers pushed the yield of solvent-based exfoliation forward to higher level. By using a sonic tip, the graphene concentration could approach ≈2 mg mL^{-1}. They also presented a modified procedure in which a pre-sonication and centrifugation process was carried out to remove unexfoliated graphite followed by redispersion and bath sonication for 24 h in NMP again.[37] The graphene concentration was as high as 63 mg mL^{-1}, with a lateral size of graphene of ≈1 μm × 0.5 μm and 3–4 layers thick on average. Though unstable, the concentration could still maintained at ≈35 mg mL^{-1} after 200 h of sedimentation. This high-concentration dispersion will benefit from practical applications such as the formation of conducting films or reinforced composites.[38]

2.1.2. Exfoliation with Low Boiling Point Solvents

Unfortunately, some disadvantages also exist for the dispersion of graphene in the aforementioned solvents, especially for good solvents such as NMP and DMF. Their high

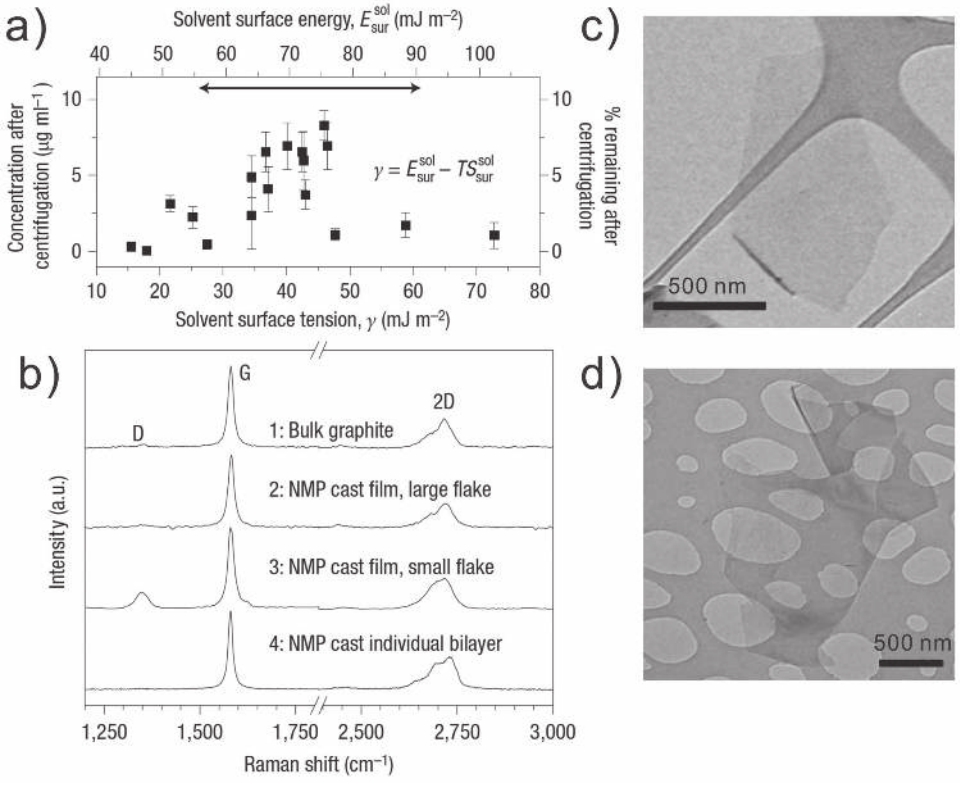

Figure 1. a) Concentration of graphene dispersions produced by various solvents plotted versus solvent surface tension. b) Raman spectra of bulk graphite and graphene flakes. c) and d) TEM images of monolayer graphene and folded graphene sheets. Reproduced with permission.[33] Copyright 2008, Nature Publishing Group.

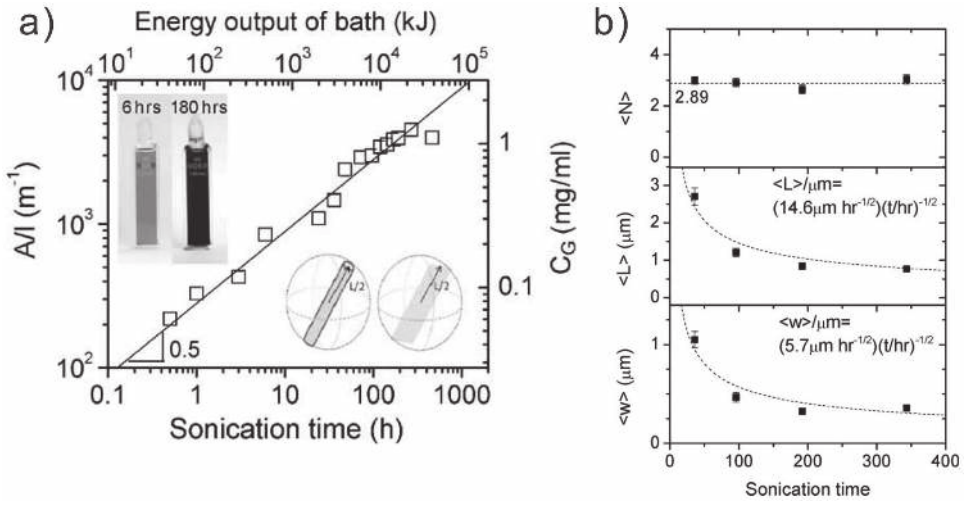

Figure 2. a) Concentration of graphene dispersion as a function of sonication time. The inset shows graphene dispersion after 6 h and 180 h. b) Mean layer number, length, and width of flakes versus sonication time. Reproduced with permission.[36] Copyright 2010, Wiley-VCH.

boiling point and toxicity hinders applications where solvent residues may greatly deteriorate the device performance. To address this issue, O'Neill et al. demonstrated that the production of graphene with a relatively high concentration and stable dispersion could be achieved with low boiling point solvents, such as isopropanol (82 °C) and chloroform (61 °C).[39] The obtained graphene flakes had dimensions of ≈1 μm × 0.35 μm on average and consisted of less than 10 layers with a higher concentration up to 0.5 mg mL^{-1} when purified at a lower centrifugation speed. Meanwhile, Choi et al. presented their work on the production of graphene in a volatile solvent, propanol, which gave a concentration of 1 mg mL^{-1}.[40] Fast evaporation of low boiling point solvents can facilitate the deposition of individual graphene flakes onto substrates without flake aggregation. In 2009, Qian and co-workers reported another low boiling point solvent, acetonitrile (ACN, 81.6 °C).[41] Assisted by a solvothermal process, sufficient energy was supplied to allow ACN molecules to overcome the potential barrier for diffusion into the interlayers of expanded graphite. After sonication and centrifugation, stable dispersion consisted of monolayer and bilayer graphene was obtained with a yield of 10–12 wt%.

Besides direct exfoliation in low boiling point solvents, a transfer method was proposed to transfer graphene dispersions from high boiling point solvents into low boiling point solvents via solvent exchange.[42] After exfoliation by NMP, graphene dispersions was filtered and re-dispersed into ethanol. By repeated filtration with ethanol for 5 times, graphene was well dispersed in a final ethanolic solution, containing ca. 0.3 vol% NMP. Compared to direct exfoliation by ethanol, the initial exfoliation in NMP with subsequent solvent exchange with ethanol shows a much better stability, although the stabilizing mechanism is not yet clear. Attempts were made in a similar way with three other solvents including methanol, dichloromethane, and toluene, however, graphene was completely precipitated after the final centrifugation.

2.1.3. Exfoliation of Other 2D Materials in Organic Solvents

Other than graphite, many other bulk layered materials could be processed with such a solvent-based exfoliation to yield good quality, high concentration and stable dispersions of 2D nanosheets. Their diverse and distinct properties are of great importance for application in electronics and energy storage. Coleman's group was the first to extend solvent-based exfoliation methods from graphene synthesis to other layered compounds, such as MoS_2, WS_2 and BN.[43] After optimization of the dispersion procedures, the concentrations of obtained 2D nanomaterials were as high as 0.3 mg mL^{-1} for MoS_2 in NMP, 0.15 mg mL^{-1} for WS_2 in NMP, and 0.06 mg mL^{-1} for BN in IPA. Statistical analyses gave the lateral size of 50–1000 nm for MoS_2 and WS_2 and 100–5000 nm for BN. Thicknesses of as-produced nanosheets were confirmed to be single layer and few layers by the analysis of TEM intensity profiles coupled with flake-edge analysis, electron diffraction patterns and electron energy-loss spectroscopy (EELS) data. In their further studies, other layered compounds such as $MoSe_2$, $MoTe_2$, $TaSe_2$, $NbSe_2$, $NiTe_2$, and Bi_2Te_3 were also synthesized by direct exfoliation in a number of solvents. The exfoliated 2D nanosheets can be easily fabricated into freestanding films, hybrids and composites, as shown in **Figure 3**a–c. The stress-stain curves in Figure 3d exhibited the mechanical reinforcement by addition of those nanosheets as fillers. Cunningham et al. performed a more comprehensive study on the dispersity of MoS_2, WS_2, $MoSe_2$, and $MoTe_2$ in twenty-one kinds of solvents.[44] The high dispersion concentration can only be obtained in solvents with matching surface energy, which is consistent with the solubility theory. Importantly, they found that the dispersion suffered an exponential decay with the Flory-Huggins parameter, as predicted by solution thermodynamics. Further research was carried out for the preparation of high concentration dispersions of exfoliated MoS_2 by long time sonication in NMP.[45] The dispersed concentration reached ≈40 mg mL^{-1}

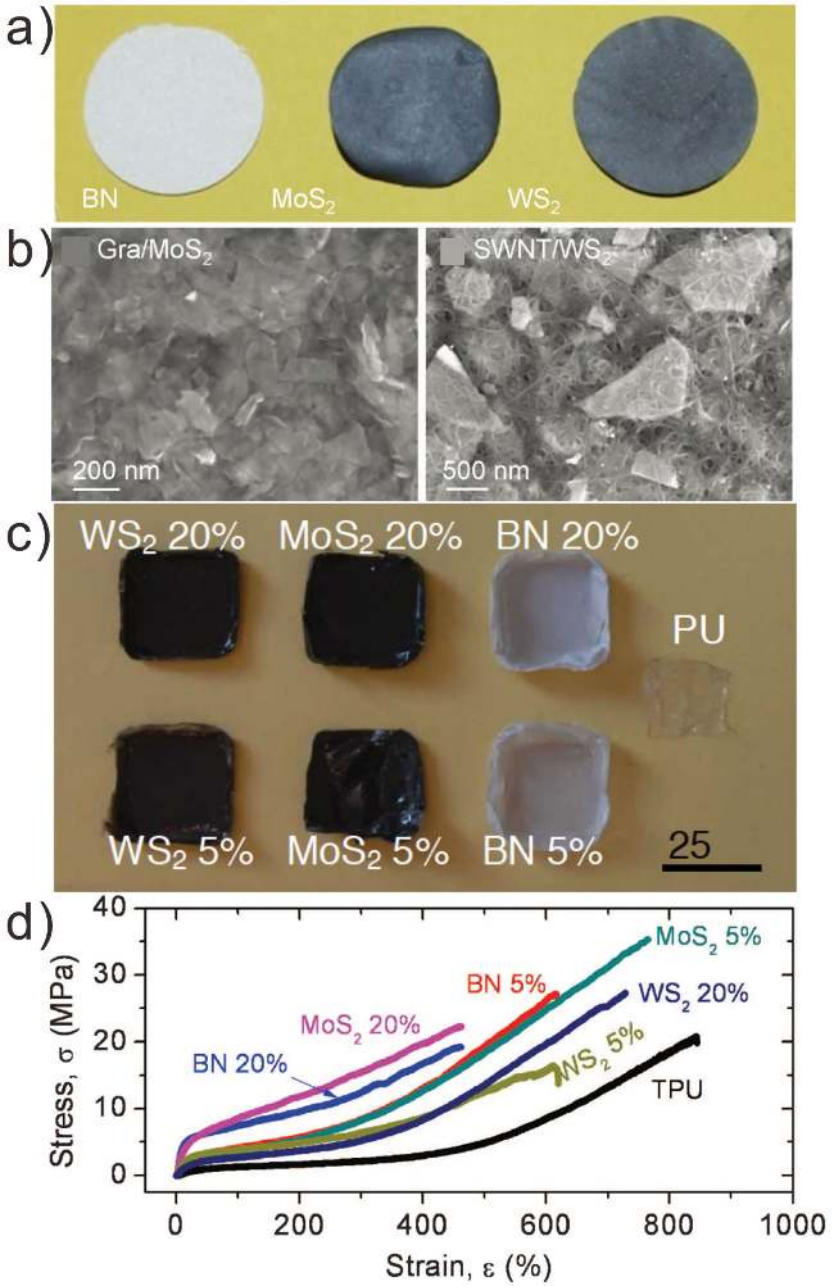

Figure 3. Representatives of a) Freestanding films, b) hybrid films, c) composites. d) Stress-strain curves for composites of polyurethane with fillers of nanosheets. Reproduced with permission.[43] Copyright 2011, American Association for the Advancement of Science.

after sonication for 200 h, however, the flake size was reduced to hundreds of nanometers because of sonication-induced scission. Relatively large flakes with a mean edge length of 2 μm can be separated by a successive process cycle: centrifugation at high speed, separation of sediments, and redispersion.[46] It is noteworthy that the addition of large flakes into polymers such as polyvinyl alcohol (PVA) exhibited enhanced performance both in strength and modulus, suggesting that MoS_2 could serve as a filler in the mechanical reinforcement of polymers. Moreover, liquid exfoliation of bulk MoS_2 powders in organic solvents in the presence of hydrogen peroxide were reported. Yun et al. argued that H_2O_2 could partially oxidize edges of MoS_2, then penetrate into interlayers, and facilitate the subsequent ultrasonic exfoliation in IPA.[47] The obtained 2D MoS_2 sheets exhibited a lateral dimension of ≈300 nm and a thickness of 1.17 nm. Dong and co-workers presented the spontaneous exfoliation of MoS_2 powders in H_2O_2-NMP mixed solvents under mechanical stirring for 10 h.[48] Besides the oxidation effect, H_2O_2 was reckoned to induce size evolution of MoS_2 nanosheets (single and few layer) from the micro- to the nanoscale.

In addition, black phosphorus (BP) has also been liquid exfoliated to give few-layered phosphorene nanosheets, which exhibit p-type semiconducting properties with a high mobility and tunable bandgap,[49–51] and are promising in optoelectronic and semiconductor-based devices.[31,49,51,52] Direct exfoliation of BP in NMP by either bath sonication[53] or tip sonication[54] has been reported to yield 2D nanosheets with thicknesses ranging from several nm to tens of nm. Yasaei et al. found that aprotic and polar solvents such as DMF and DMSO, among several investigated solvents, were appropriate for the synthesis of stable and uniform dispersion of phosphorene nanosheets.[55] Note that the exfoliated BP degrades upon the exposure to water and oxygen, limiting its potential application,[56,57] Hanlon et al. studied the exfoliation of BP in N-cyclohexyl-2-pyrrolidone (CHP) and proposed that the solvation shell of solvent molecules could protect exfoliated nanosheets from reacting with water.[58] Organic solvent-assisted exfoliation is also true of layered metal oxides. Multilayer MoO_3 nanosheets with good quality were prepared by liquid exfoliation of layered crystallites in solvents, such as CHP and NMP.[59] By combination with CNTs, the supercapacitors displayed a capacitance up to 540 F g^{-1} at 0.1 mV s^{-1}.

2.2. Stabilizer-Based Exfoliation

Although direct exfoliation in organic solvents is simple and straightforward, their use is less environmentally friendly. To address this issue, another strategy has been developed to exfoliate bulk layered crystals in liquid media with the assistance of stabilizers including surfactants, polymers and pyrene derivatives. The use of a stabilizer can effectively tune the surface tension of the aqueous solution so as to allow efficient exfoliation. This

section is arranged to review related works by the kind of stabilizer used.

2.2.1. Ionic Surfactants

Graphite powder was sonicated in aqueous solutions of sodium dodecylbenzene sulfonate (SDBS).[60] TEM analysis revealed graphene sheets with a lateral size of 0.1–3 μm and a thickness distribution of ≈3% monolayer and ≈43% <5 layers. FTIR and Raman results showed that a small amount of oxidation occurred in the exfoliation/dispersion process, which was ascribed to edge defects. The dispersion concentration could approach 0.1 mg mL^{-1}. The dispersion was stabilized by electrostatic repulsion for over 6 weeks before large flakes started to precipitate. Relatively conductive thin films (30 nm) were fabricated via vacuum filtration followed by annealing at 250 °C, exhibiting a sheet resistance of 22.5 kΩ sq^{-1} and a conductivity of 1500 S m^{-1}. Coleman's group later presented the use of sodium cholate (SC),[61] with which the dispersion concentration could be increased up to 0.3 mg mL^{-1} by long time sonication (400 h). TEM analysis revealed that those graphene nanoflakes were typically ≈4 layers with length and width of ≈1 μm and ≈400 nm, respectively, up to 20% of which were single layer. The dispersion can be easily cast onto high-quality films. Films fabricated by De et al. showed an improved conductivity of 1.5×10^4 S m^{-1} after annealing at 500 °C.[62] The sheet resistance was less than 10^4 Ω sq^{-1} with an optical transmittance of ≈80%. Green and co-workers also reported similar results, where they used the density gradient ultracentrifugation (DGU) technique to isolate graphene sheets with controlled thickness. Compared with sedimented centrifugation, the performance of films fabricated from DGU were improved in the sheet resistance and transmittance.[63] Hasan et al. exfoliated the graphite powders by mild sonication in aqueous solution of sodium deoxycholate (SDC) bile salt.[64] Compared to an SC-assisted exfoliation process, they argued that SDC could form denser and more regular coverage; therefore dispersion of SDC-graphene would be more stable. This is because the hydrophobic index of SDC is higher than SC, which strongly improves its absorption on graphitic surfaces. Hao et al. introduced 7,7,8,8-tetracyanoquinodimethane (TCNQ) anion as a stabilizer to prepare graphene aqueous dispersion by using expanded graphite[16] as the starting material.[65] TCNQ can be absorbed onto the graphene surface by π–π stacking interactions; moreover its negative charge can prevent exfoliated graphene sheets from aggregation via electrostatic repulsion. Though single- and few-layered graphene sheets with few defects were obtained, the dispersion concentration was quite low, being only 15–20 μg mL^{-1}. Nevertheless, the excellent electrical and magnetic properties for both TCNQ and graphene may show unique physical performances for TCNQ-graphene composites.

In general, surfactants comprise a hydrophobic tail group and a hydrophilic head group. Specifically, for ionic surfactants, the tail groups can absorb non-polar objects via various interactions such as van der Waals interactions and hydrophobic interactions; while the head groups are prone to dissociation, charging the flakes. Therefore, surfactant-coated graphene flakes are stabilized by the electrostatic repulsion between each other. The electric potential of aqueous dispersions can be approximately characterized by the zeta potential, ζ. The dispersion concentration scales with the square of the zeta potential, which stabilizes the surfactant-coated graphene sheets against aggregation.

In addition to graphite, surfactant-assisted exfoliation has also been extended to other layered inorganic compounds, such as BN, MnO_2 and TMDs. Smith and co-workers probe-sonicated layered crystals in aqueous solutions of SC.[66] The 2D nanosheets were stabilized in aqueous solutions due to the van der Waals binding with stabilizers and the subsequent electrostatic interaction (**Figure 4**a). TEM characterization revealed well-dispersed 2D nanosheets comprising a few layers (Figure 4b–g). Hybrid thin films made of MoS_2 and SWNT have exhibited promising results in thermoelectric research and Li-ion battery research.

Apart form the aforementioned anionic surfactants, some attempts have also been made using cationic surfactants. Vadukumpully and co-workers demonstrated the preparation of few-layered graphene flakes via mild sonication of highly ordered pyrolytic graphite (HOPG) in the presence of cetyltrimethylammonium bromide (CTAB) and acetic acid.[67] The tail group of long alkyl chains could adsorb onto the graphene surface through hydrophobic interactions and the electrostatic charge could prevent restacking and agglomeration. Statistical analysis revealed that the thickness of the graphene flakes was 1.18 nm with ≈85% <4 layers. The average lateral size was 0.7 μm × 0.5 μm. A total yield of ≈10% was obtained. To further improve the dispersion concentration, Notley proposed ultrasonic exfoliation with the continuous addition of surfactants, in contrast to previously reported single addition prior to sonication.[68] During the sonication process, the surface tension of the solution increased over time due to the consumption of bulk surfactant. By continuous addition of surfactants, the surface tension could be maintained at an optimum value (≈41 mJ m^{-2}) for efficient exfoliation, thereby significantly increasing the dispersion concentration up to 15 mg mL^{-1} (Figure 4i). This strategy was confirmed by using other types of surfactants, either ionic or non-ionic.

2.2.2. Nonionic Surfactants

Non-ionic surfactants tend to stabilize the graphene dispersion better than ionic ones, probably due to the more efficient steric repulsion than electrostatic repulsion.[69] Guardia and co-workers presented the preparation of graphene aqueous dispersion in a wide range of non-ionic surfactants in comparison with several ionic ones via direct bath sonication in water (**Figure 5**). Apparently, the concentration of graphene dispersion obtained from non-ionic surfactant was much higher. For the most effective non-ionic surfactant, P-123, the concentration approached 0.9 mg mL^{-1}, which could be further increased to ≈1.5 mg mL^{-1} after prolonging the sonication duration to 5 h. These dispersions were processed into paper-like films with highest electrical conductivity of

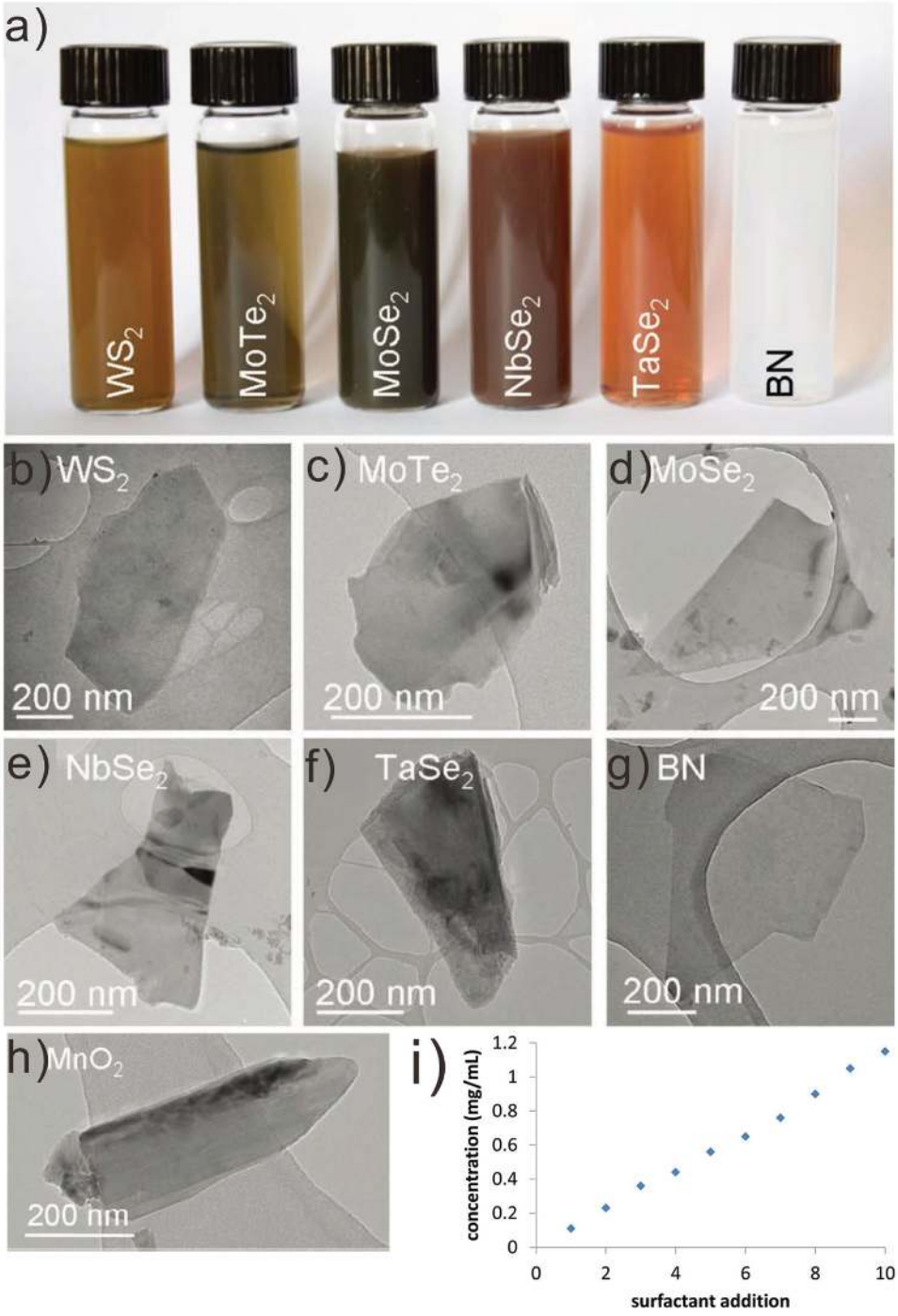

Figure 4. a) Dispersion of exfoliated layered compounds, b-h) TEM images of exfoliated 2D nanosheets. Reproduced with permission.[66] Copyright 2011, Wiley-VCH. i) Increased concentration of graphene dispersion upon the continuous addition of surfactant. Reproduced with permission.[68] Copyright 2012, American Chemical Society.

3600 S m^{-1}, but larger fraction of surfactant in the films led to lower conductivity. Geng et al. reported the successful exfoliation of graphite in NMP containing nonionic porphyrin.[70] It might involve a two-step process: organic ammonium ion intercalation and porphyrin induced exfoliation via π–π interactions with graphene. The obtained graphene sheets exhibited undisturbed sp^2 carbon networks.

The stabilization mechanism of non-ionic surfactants may be attributed to steric effects because the hydrophobic tail absorbs on graphene sheets while the long hydrophilic part spreads into water. Once the graphene sheets approach close to each other, the protruding head groups will interact to induce osmotic repulsion. Smith and co-workers selected 12 representative surfactants consisting of ionic and non-ionic types to discuss in detail the stabilization mechanism in surfactant-assisted graphite exfoliation.[71] The outcome demonstrated that the dispersion concentration scaled linearly with the steric repulsive potential barrier.

List of surfactants &their acronyms used in the text

Surfactant name	Acronym
Non-ionic	
Pluronic® P-123	P-123
Tween 80	
Brij 700	
Gum arabic from acacia tree	
Triton X-100	
Tween 85	
Brij 30	
Polyvinylpyrrolidone	PVP
n-Dodecyl β-D-maltoside	DBDM
Ionic	
Poly(sodium 4-styrenesulfonate)	PSS
3-[(3-Cholamidopropyl)dimethyl ammonio]-1-propanesulfonate	CHAPS
Sodium deoxycholate	DOC
Sodium dodecylbenzene-sulfonate	SDBS
1-Pyrenebutyric acid	PBA
Sodium dodecyl sulphate	SDS
Sodium taurodeoxycholate hydrate	TDOC
Hexadecyltrimethylammonium bromide	HTAB

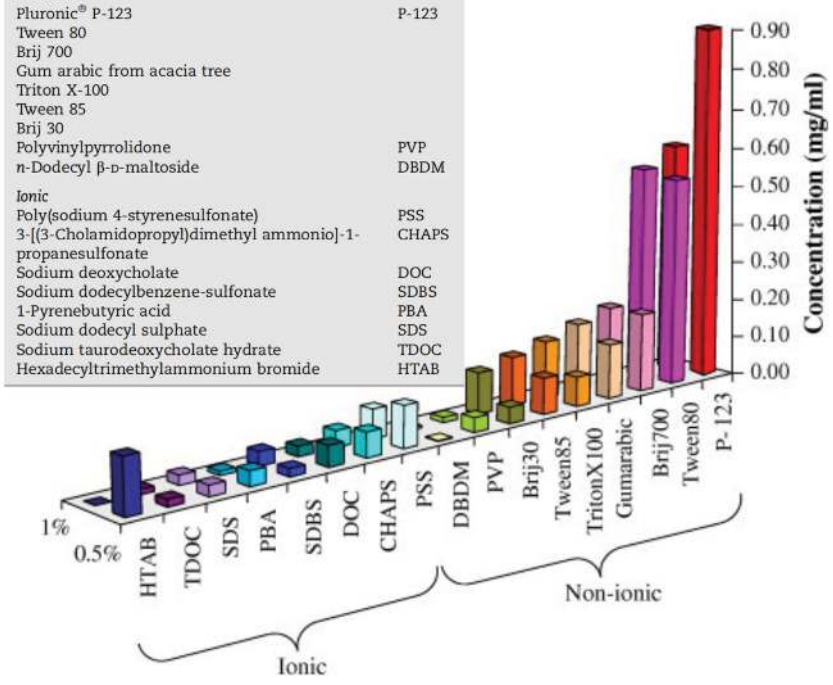

Figure 5. Concentration of graphene dispersions obtained by various types of surfactants. Reproduced with permission.[69] Copyright 2011, Elsevier.

2.2.3. Polymers

Graphite was also exfoliated in water or organic solvents with the aid of polymers, such as polystyrene (PS), PVC and poly(methyl methacrylate) (PMMA). Bourlinos et al. presented the synthesis of crystalline and non-oxidized graphene by direct sonication of graphite powders in aqueous phases in the presence of a non-toxic polymer, polyvinylpyrrolidone (PVP).[72] The choice of PVP is based upon the following merits: biocompatibility and safety, solubility in water, affinity to graphite surfaces, and post-immobilization activity of other molecular species. The results showed that the graphene sheets (0.1 mg mL^{-1}) were few-layered with few defects. The stabilization mechanism of PVP-graphene can be considered in the viewpoint of steric or depletion effects. Water-soluble biopolymer such as protein albumin was also attempted, which gave a concentration of 0.15–0.2 mg mL^{-1}. Liang et al. reported efficient graphene exfoliation in ethanol with the addition of a stabilizing polymer, ethyl cellulose (EC).[73] The dispersion was further concentrated from 122.2 μg mL^{-1} to 1.02 mg mL^{-1} via iterative solvent exchange. In the mixture of terpineol and EC-stabilized graphene-ethanol soltuion, graphene was preferentially concentrated into a terpineol fraction. Transparent conductive thin films were fabricated, exhibiting sheet resistance of several to hundreds of kΩ sq^{-1} with a transmittance of ≈70–90%.

May and co-workers carried out a statistical study to figure out what kind of polymer-solvent combinations could exfoliate and stabilize layered nanomaterials,[74] which might be of great use for applications in fabricating polymer/2D nanomaterials composites. The exfoliation of bulk crystals of graphite, h-BN, and MoS_2 was performed in a range of polymers dissolved in two different solvents. A simple model was established in terms of Hildebrand solubility parameters of nanosheets, polymer and solvent. When these materials had similar solubility parameters, the dispersion of exfoliated nanosheets could be obtained, however, the concentration was too low, on a scale of μg mL^{-1}. Later, Xu and co-workers reported the production of graphene dispersions with increased concentration by a solvent/polymer pair: tetrahydrofuran (THF) (or $CHCl_3$)/hyperbranched polyethylene (HBPE).[75] In the exfoliation process, absorbed HBPE on graphene flakes provided steric stabilization against restacking. TEM, atomic force microscopy (AFM) and Raman spectroscopy characterizations showed that graphene flakes were defect-free, and few-layered (2–4 layers), with a lateral size of 0.2–0.5 μm. The concentration of dispersion in chloroform was 0.18 mg mL^{-1}, which could be concentrated to 3.4 mg mL^{-1} by solvent evaporation.

Beyond the stabilization effect in the exfoliation process, polymers could also be used to modify graphene wettability. Skaltsas et al. reported the switched solubility of graphene from the organic to aqueous phase by adding amphiphilic block copolymers, such as poly[styrene-*b*-(2-vinylpyridine)] (PS-*b*-P2VP) and poly(isoprene-*b*-acrylic acid) (PI-*b*-PAA).[76] The graphene dispersion was prepared by tip sonication in NMP or o-dichlorobenzene, however, the graphene quality was poor: a concentration of several μg mL^{-1}, a small lateral size of ≈50 nm, and thick layers of 1.5–20 nm.

2.2.4. Pyrene Derivatives

Generally, larger concentrations of small molecular surfactants and polymers will lead to high a dispersion concentration of graphene nanosheets. However, difficulties of removal of excessive stabilizer in dispersion may impose negative effects on the performance of films, composites and electronic devices. Therefore, the search for alternative stabilizers that can stabilize large amount of graphene sheets at low concentrations is necessary. Polycyclic aromatic hydrocarbons (PAH) such as pyrene (Py) and its derivatives (**Figure 6**) show great promise in this respect due to π–π interactions between the planar surfaces of stabilizer and graphene.[77–84]

For instance, Dong et al. showed the effective exfoliation of graphite into monolayer graphene with the aid of tetrasodium 1,3,6,8-pyrenetetrasulfonic acid (Py-$4SO_3$) via probe sonication.[84] Statistical analysis of AFM images indicated

most exfoliated graphene sheets were monolayer. From Raman spectra, graphene sheets sandwiched by Py-4SO_3 molecules exhibited a pronounced G band splitting. An et al. prepared graphene aqueous dispersion in the presence of 1-pyrenecarboxylic acid (PCA).[153] Graphene Films made by vacuum filtration were integrated into chemical sensors with a rapid resistance change of 10000% in saturated ethanol vapor and ultracapacitors with high capacitance of ≈120 F g^{-1}. Similarly, Zhang et al. reported the production of high quality and monolayer graphene sheets via the sonication of graphite powders in aqueous solutions of pyrene molecules functionalized with water-soluble groups, including Py-NH_2 and Py-4SO_3.[78]

Beyond the stabilization effect, pyrene molecules could also act as the nanographene to heal the possible defects existing in graphene sheets. After 1000 °C annealing, transparent conductive films made with Py-SO_3 exhibited a conductivity of 181200 S m^{-1}, sheet resistance of 778 Ω sq^{-1} and 90% transmittance in the visible light range. Jang and coworkers reported a novel one-pot in situ supercritical fluid exfoliation with 1-pyrene sulfonic acid sodium (Py-1SO_3) in mixed solutions of ethanol/water.[83] Py-1SO_3 molecules absorbed on graphene surface acted as electron-withdrawing groups leading to an electron transfer from graphene nanosheets to Py-1SO_3 molecules, which was confirmed by the red shift of G peak in the Raman measurement. The presence of Py-1SO_3 molecules not only increased the yield of monolayer and bilayer graphene sheets (60%), but also improved the Li-ions storage capacity. Although Yang and co-workers also reported the use of Py-1SO_3 for the graphite exfoliation, their method seemed more superior and straightforward, just by bath sonication of graphite flakes in aqueous solution of Py-1SO_3.[82] The dispersion concentration was ≈0.07 mg mL^{-1} with a lateral size less than 1 μm. Apart from those simple functionalized pyrene derivatives mentioned above, Lee et al. designed an aromatic amphiphile molecules consisting of an aromatic segment based on four pyrene units and a hydrophilic dendron, which could selectively assemble onto graphene surfaces via non-destructive π–π stacking interactions and consequently facilitate the dispersion of graphene sheets in aqueous solution.[79] A higher concentration up to 1.5 mg mL^{-1} was obtained by direct sonication in H_2O/methanol.

Nevertheless, existing literature falls short of detailed studies on pyrene derivatives in terms of the impact of stabilizer concentration, functional groups, and counterions. Parviz and co-workers listed pyrene derivatives with various functional groups (Figure 6), which would affect the formation and strength of π–π interactions, thereby determining the dispersion yield of graphene sheets.[80] First of all, compared with surfactant and polymer systems, pyrene derivatives of lower concentrations can take effect in stabilizing graphene dispersions. Secondly, among all the presented pyrene derivatives, Py-1SO_3 was the most effective to yield graphene concentration up to 0.8–1 mg mL^{-1}. Thirdly, regarding the role of functional groups in pyrene derivatives, it was found that functional groups with higher electronegativity were more efficient in the adsorption of

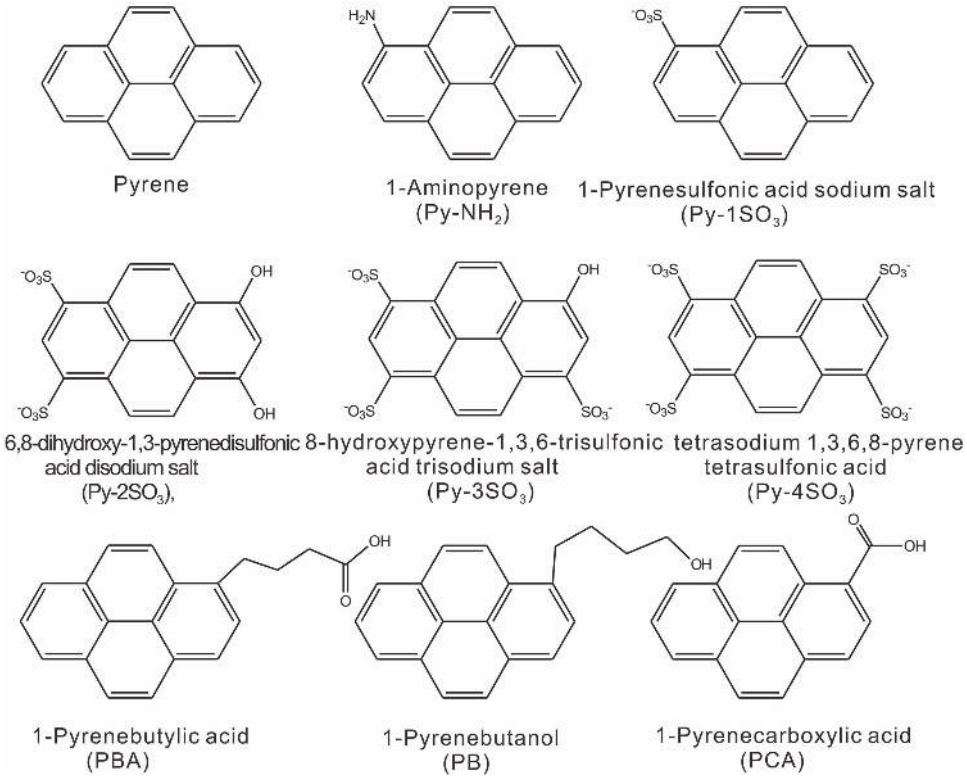

Figure 6. Chemical structures of pyrene derivatives used as the stabilizers in the liquid based production of 2D nanomaterials, with their names and corresponding acronyms.

stabilizers onto graphene surface. Meanwhile the number of functional groups, arrangement on the basal plane and their distance from the pyrene molecules should be optimized to facilitate the dispersion. Moreover, pyrene derivatives with sulfonyl groups could produce more stable dispersion over a wide range of pH, while the rest would be stable at certain pH values. Further to the said work for the molecular understanding of the interactions between graphene and aromatic dyes, Schlierf and co-workers performed comparative studies by successive exfoliation of graphite in aqueous solutions of different pyrene sulfonic acid sodium salts, including Py-1SO_3, 6,8-dihydroxy-1,3-pyrenedisulfonic acid disodium salt (Py-2SO_3), 8-hydroxypyrene-1,3,6-trisulfonic acid trisodium salt (Py-3SO_3) and Py-4SO_3.[81] By combining experimental and modeling investigations, the correlation between graphene-dye interaction energy, the molecular structure and the amount of solubilized graphene flakes were unveiled. The results indicated that the molecular dipole was not important per se, but because it facilitated adsorption on graphene by a "sliding" mechanism of the molecule into the solvent layer, promoting lateral displacement of water molecules collocated between aromatic cores of the organic dye and graphene.

2.2.5. Other Stabilizers

Other than pyrene and its derivatives, more polycyclic aromatic hydrocarbons are introduced to exfoliate graphite into single- and few-layered graphene sheets, such as perylenebisimide-based bolaamphiphile detergent[154] and tetrapotassium salt of coronene tetracarboxylic acid.[155] Being highly water-soluble, they can act as the acceptor molecules and the large planar aromatic surface allows the strong interactions with graphene surface via synergistic noncovalent charge-transfer and π–π stacking interactions. Furthermore, the negative charge can prevent inter and intra re-stacking of graphene sheets, leading to the good stabilization of graphene dispersions.

2.3. Ionic Liquid-Based Exfoliation

Ionic liquids (ILs) are semiorganic salts with a melting point below 100 °C. Due to the unique properties such as high ionic conductivity, good thermal stability, nonflammability, and low vapor pressure, ILs have attracted much attention.[156] Inspired by the use of ILs in the dispersion of carbon nanotubes,[157] One can expect that ILs can also be used in the stabilization of graphene nanosheets via Coulombic interaction. Wang et al. demonstrated the direct exfoliation of graphite flakes via tip sonication in ILs, such as 1-butyl-3-methylimidazolium bis(trifluoromethanesulfonyl)imide ([Bmim][Tf2N].[85] This method yielded stable few-layered graphene suspensions of ≈0.95 mg mL^{-1} and a lateral size of micrometers. Nuvoli et al. further increased the concentration of graphene dispersion up to 5.33 mg mL^{-1} by direct sonication in another IL, 1-hexyl-3-methylimidazolium hexafluorophosphate (HMIH).[86]

2.4. Salt-Assisted Exfoliation

The liquid exfoliation in organic solvents of stabilizer-based aqueous solutions generally requires sonication for a long time, yet has a low yield. To address these challenges, Zheng's group reported a modified liquid-phase ultrasonic exfoliation method, which made use of inorganic salts.[87,88] In this method, powders of layered crystals, such as graphite and TMDs, were immersed into inorganic salts-containing aqueous solution, and salt ions were allowed to enter and precipitate into interlayer spacings as the solution supersaturates upon water evaporation. The intermediate products were then easily exfoliated into single- and few-layered 2D nanosheets by lower power ultrasonic bath in organic solvents. More than 65% of the as-made products comprised a few layers (1–5 layers) with a lateral size ranging from a few hundred nm to tens of μm, which appeared to be related to the size of the starting materials. More importantly, the sonication time was dramatically shortened to 2 h and when compared to direct sonication in organic solvents without the addition of salts, the yield was increased as high as 32-fold.[88] The exfoliated MoS_2 nanosheets were solution-casted into thin films to serve as the hole transport layer in organic solar cells.

2.5. Intercalant-Assisted Exfoliation

2.5.1. Li^+ Intercalation

The presence of intercalants such as Li ions and organic molecules could facilitate the exfoliation of bulk layered crystals into 2D nanomaterials. This is because after the insertion, the interlayer spacings of bulk layered crystals are dramatically expanded and the interlayer interaction is greatly weakened, accordingly. Therefore layered materials can be more easily exfoliated upon the subsequent ultrasonication.

Li^+ intercalation of the layered TMDs via n-butyl lithium (BuLi) has been studied.[89] In 1986, Joensen et al. reported the synthesis of single-layered MoS_2 by using BuLi.[90] This reaction process involved the intercalation of Li^+ by soaking MoS_2 powders in the hexane solution of BuLi for 48 h and subsequent reaction of the dried intermediate product with water, which can be described by the following equations:[91]

$$MoS_2 + BuLi \rightarrow LiMoS_2 + 1/2Bu\text{-}Bu \quad (1)$$

$$LiMoS_2 + xH_2O \rightarrow MoS_{2(monolayer)} + xLiOH + \frac{x}{2}H_2 \quad (2)$$

The released gaseous hydrogen can force the layers apart. X-ray diffraction patterns, which were consistent with the theoretically calculated MoS_2 patterns with one molecular layer, confirmed the synthesis of single-layered MoS_2 sheets. This product could be used to produce novel polymer/MoS_2 nanocomposites.[91]

This strategy has been applied to other layered materials. For example, Miremadi et al. reported the exfoliation of WS_2.[92,93] Unfortunately, Li ions were difficult to completely intercalate for efficient exfoliation, possibly because

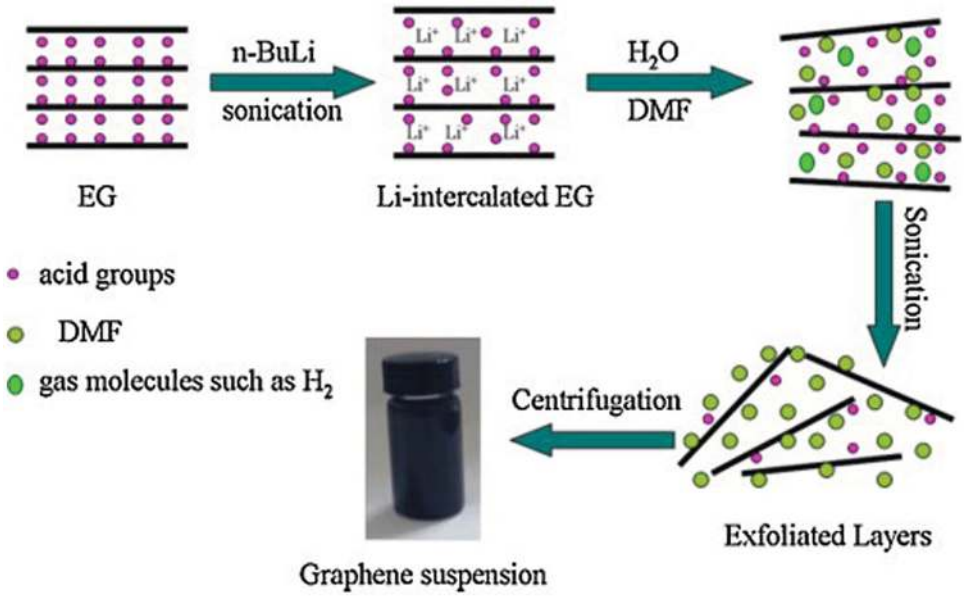

Figure 7. Scheme of n-butyl lithium assisted exfoliation and dispersion of graphene sheets in DMF. Reproduced with permission.[96] Copyright 2013, Elsevier.

of the formation of an oxide, which might seal the edges against intercalation. Therefore, this method was modified by sequential ultrasonication of WS_2 powders in pure hexane and in hexane solution of BuLi overnight. The energy derived from the ultrasonic treatment was proposed to induce the slippage between basal planes, facilitating the penetration of Li^+. However, the exfoliated sheets restacked easily during filtration. The addition of some ions (e.g., Ni^{2+}, Al^{3+}) or acids could stabilize the dispersion of single sheets due to the induced flocculation. Tsai and co-workers simply modified this method by reacting $LiBH_4$ with WS_2 to form intercalated $LiWS_2$ followed by exfoliation in water to produce single-layered sheets.[94]

In order to study the physical and structural properties of single layered dichalcogenides, Gordon et al. performed the intercalation and exfoliation process with BuLi.[95] Three-dimensional models of the structures of single-layered nanosheets such as MoS_2, $MoSe_2$ and WS_2 were obtained by using X-ray absorption fine structure (XAFS) and XRD. The results showed that single-layered nanosheets possessed a 2D rectangular unit cell rather than the hexagonal cell of their bulk counterparts. Moreover, Zhou et al. presented a liquid phase exfoliation via ultrasonication of the mixture of expandable graphite (EG) and BuLi in hexane followed by ultrasonic exfoliation of Li-intercalated intermediate products in a water/DMF solution.[96] EG derived from concentrated sulfuric acid treatment resulted in partial oxidation at edges and defective sites, which led to negative charges of the graphene layers and facilitated the Li^+ intercalation. Subsequently, the rapid hydrolysis of Li-intercalated EG produced few-layered graphene sheets (**Figure 7**). EG samples of different sizes were studied, with smaller sizes able to produce thinner graphene sheets, possibly due to weaker van der Walls interactions in smaller sizes of EG. Note that this Li-assisted exfoliation has drawbacks due to its sensitivity to ambient conditions; therefore more attention should be paid to the intercalation process, which is normally conducted in an inert gas-filled glovebox.

2.5.2. Acid Intercalation

For decades, the intercalation of bulk layered materials has been thought to be driven by redox reactions involving host-guest charge transfer processes.[97] This may result in the partial oxidation, reduction or covalent modification of exfoliated 2D nanosheets.[98] Insulating BN is not susceptible to oxidative intercalation except by extremely strong oxidizing agents. Kovtyukhova et al. reported the reversible and nonoxidative intercalation of h-BN by thermal drying of suspensions of h-BN with Bronsted acids including H_2SO_4, H_3PO_4, and $HClO_4$ to form stage-1 compounds.[158] This tendency has also been observed in the intercalation of graphite and TMDs. Later, Kovtyukhova et al. experimentally studied the intercalation of graphite by using Bronsted acids.[98] It is suggested that this process was initiated by activation of the outermost host layers by acid–base rather than electron transfer reactions and the guest molecule activity must exceed a threshold for the bulk intercalation to start. The intercalated compounds could be readily exfoliated in DMF to give single- and few-layered graphene suspensions.

2.5.3. Organic Molecule Intercalation

A variety of organic molecules has been used to intercalate the layered materials to facilitate the exfoliation process. Recently, a new group of 2D materials, called MXenes, was produced via selective etching of an A-group element (by aqueous hydrogen fluoride) from layered ternary MAX phases (general formula of $M_{n+1}AX_n$) such as Ti_3AlC_2, where

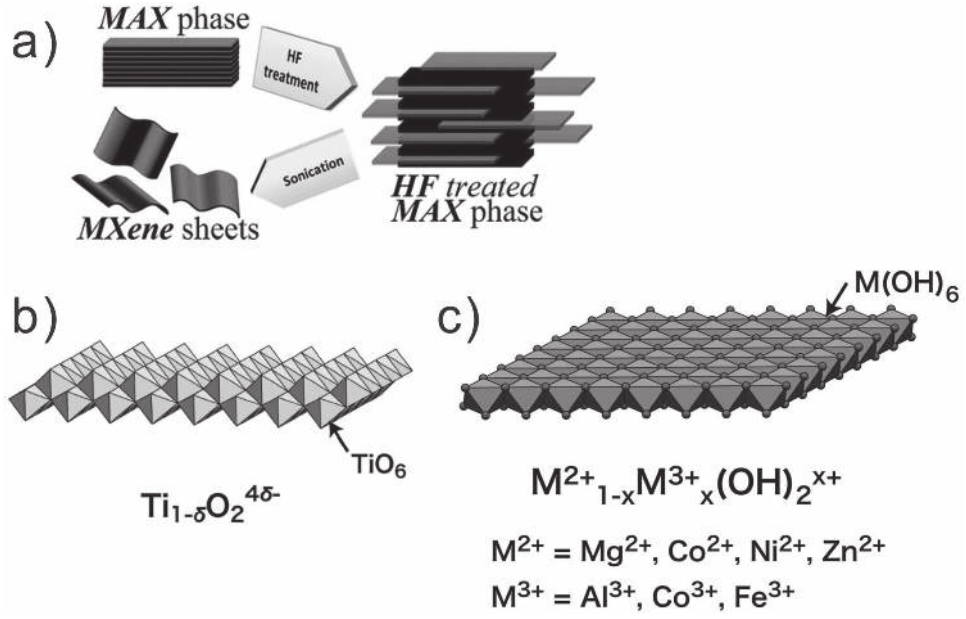

Figure 8. a) The exfoliation process of MAX phase and foramtion of 2D MXene nanosheets. Reproduced with permission.[3] Copyright 2012, American Chemical Society. b,c) Representative structures of metal oxide and hydroxide nanosheets. Reproduced with permission.[101] Copyright 2010, Wiley-VCH.

M is an early transition metal, A is an A-group element (mainly groups 13 and 14), and X is C or N.[4,99] **Figure 8**a schematically shows the exfoliation process. After removal of the A element, the weak bonds between OH and/or F-terminated MX layers allow the intercalation of different species (organic, inorganic, and ionic). Mashtalir et al. reported that the intercalation of hydrazine, hydrazine dissolved in DMF, DMSO, and urea into Ti_3C_2 resulted in the increase of c-lattice parameters, clarified by XRD mearsurements.[100] The intercalation of DMSO enabled the delamination of stacked layers into separate 2D MXene flakes upon weak sonication in deionized water. Because of the conductive and hydrophilic nature of 2D MXene nanosheets,[101] they are very promising electrode materials for application in Li-ion batteries,[102,103] supercapacitors,[104–108] and other batteries.[109,110]

2.6. Ion Exchange-Based Exfoliation

This method refers to the exfoliation of a class of special layered materials, which contains an ion-exchangeable interlayer, such as cation-exchangeable metal oxides (e.g., TiO_2) and anion-exchangeable layered double hydroxides (LDH). Figure 8b and 8c show the representative structures of metal oxide and hydroxide nanosheets, possessing mixed valence. For layered metal oxides, the intercalation of bulky organic ions, e.g., quaternary ammonium and tetrabutylammonium cations[111] could weaken the electrostatic interaction between the host layers and the cationic interlayer species, facilitating the subsequent exfoliation with the aid of weak shear force. Regarding Layer double hydroxides, they have a general formula $[M^{2+}_{1-x}M^{3+}_{x}(OH)_2](A^{n-})_x/n\ mH_2O$, in which M^{2+}, and M^{3+} represent respectively divalent and trivalent metal ions, and A^{n-} represents the charge-balancing anion. It has been reported that simple inorganic anions (e.g., NO_3^-)[112] or organophilic anions (long-chain carboxylates or other anionic surfactant, e.g., $C_{12}H_{25}OSO_3^-$)[113] could be incorporated into the interlayers of bulk LDH to assist the exfoliation. Moreover, the solvation in organic solvents, such as formamide,[93] and butanol, under ultrasonication could also achieve the exfoliated nanosheets. These charge-bearing nanosheets can be assembled via different solution-based techniques to form films, composites and core-shell structures, which will benefit the applications in electrical, magnetic, optical and catalytic fields.[3,114,115]

3. Electrochemical Exfoliation

Unlike the direct ultrasonic exfoliation method that typically requires a longer time (several days), the electrochemical exfoliation of bulk layered materials in a two-electrode system can be accomplished on the order of minutes to hours. Beyond that, more advantages can be expected, such as relatively simple operation processes, straightforward performance in ambient conditions, and production on the scale of milligrams to grams.[159] The basic concept of electrochemical exfoliation is to intercalate ionic species into bulk layered materials under an electrochemical bias, and to facilitate the subsequent ultrasonic exfoliation. The ionic species responsible for the intercalation can be anionic or cationic. These are considered in turn in the following sections.

3.1. Anionic Intercalations

The experimental setup for electrochemical exfoliation with anionic species involves using a bulk layered material as the anode and another material (such as Pt) as the counter electrode. The first example of this kind was demonstrated with a

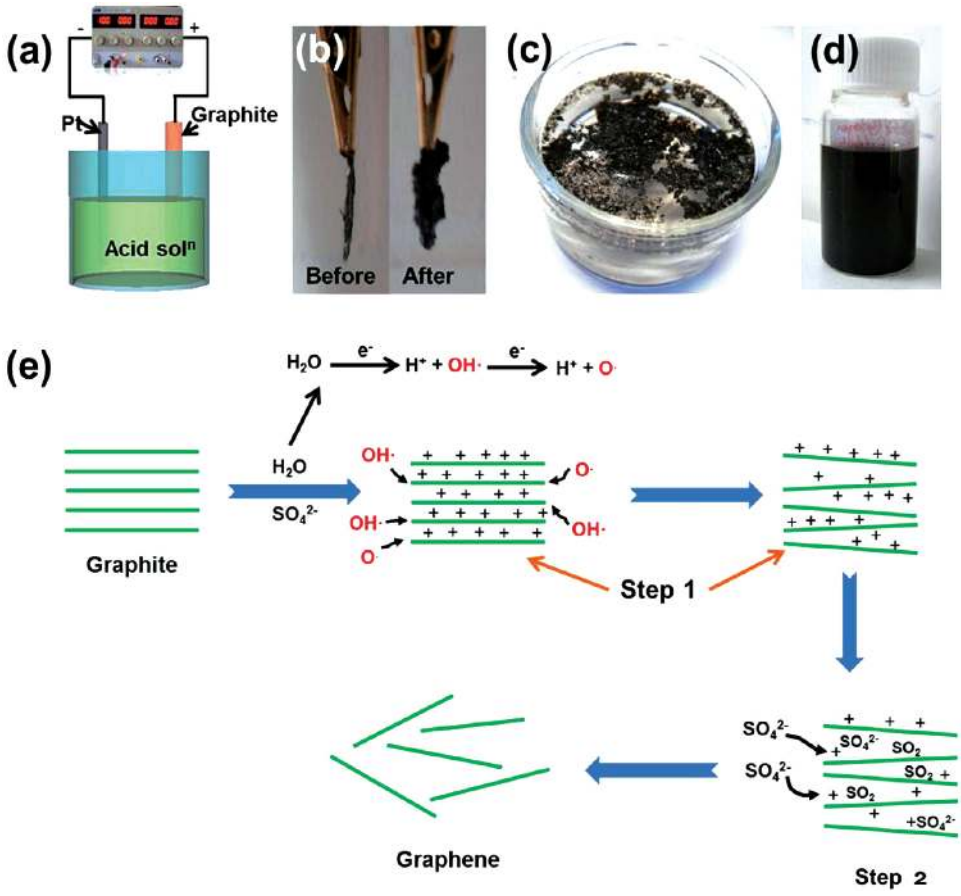

Figure 9. a) Schematic illustration of electrochemical exfoliation of graphite in acid solution. b) Photos of graphite flakes before and after exfoliation. c) Exfoliated graphene floated on top of water. d) Dispersed graphene sheets in DMF. e) Proposed mechanism for electrochemical exfoliation. Reproduced with permission.[117] Copyright 2013, American Chemical Society.

graphite anode and Pt cathode with different electrolyte solutions (**Figure 9**a). Su et al. demonstrated the high-speed electrochemical exfoliation of graphite into graphene sheets in H_2SO_4-KOH solutions.[116] In this work, electrolytes containing various acids, such as HBr, HCl, HNO_3 and H_2SO_4, were investigated, but only H_2SO_4 was found effective. The addition of KOH was used to attenuate the strong oxidation effect of H_2SO_4, which would generate defects in exfoliated graphene sheets. The presence of the D band in Raman spectra and functional groups in XPS confirmed the existence of defects in graphene sheets. However, this method could produce thin graphene sheets, 65% of which were less than 2 nm with a lateral size of 1–40 μm. This large size could facilitate the fabrication of percolative graphene thin films with an excellent conductivity of 210 Ω sq^{-1} and a transparency of 96%. The filed-effect mobility of a single graphene sheet was up to 17 $cm^2 V^{-1} s^{-1}$.

Parvez et al. reported a similar work, but in a more acidic solution, in which graphite was electrochemically exfoliated in 0.1 M H_2SO_4 aqueous solution (Figure 9e).[117] The oxidation of water under bias voltage generated hydroxyl and oxygen radicals, which would induce oxidation and hydroxylation to edge sites and grain boundaries of graphite electrode. The defective sites could facilitate the intercalation of SO_4^{2-} into graphite interlayers. Subsequently, the expansion of interlayer spacing occurred due to the release of gaseous SO_2 or anion depolarization. The optimized electrolyte concentration produced high yield (>80%) of graphene sheets with 1–3 layers and low sheet resistance of 4.8 kΩ sq^{-1} for a single flake. These patterned graphene films were demonstrated to serve as high performance source/drain electrodes for organic filed-effect transistors.

In addition, Parvez et al. also reported the electrochemical exfoliation of graphite in aqueous solutions of various inorganic salts, such as Na_2SO_4 and K_2SO_4.[118] The obtained graphene sheets showed a high yield of 85% (≤ 3 layers) with a lateral size up to 44 μm and a high hole mobility of 310 $cm^2 V^{-1} s^{-1}$. Highly conductive graphene films (11 Ω sq^{-1}) were fabricated on A4 paper by brush painting of graphene ink. Solid-state flexible supercapacitors were demonstrated with these highly conductive graphene materials, exhibiting an areal capacitance of 11.3 mF cm^{-2}. Salts containing SO_4^{2-} showed apparent exfoliation efficiency, whereas other anions such as Cl^-, NO_3^- and ClO_4^- had no obvious effects. This method avoids over-oxidation through the use of acidic electrolytes. Recently, bulk MoS_2 was also electrochemically exfoliated in Na_2SO_4 electrolyte.[119] A similar exfoliation mechanism was proposed as depicted in Figure 9e. The MoS_2 nanosheets were redispersed in NMP with a concentration of 0.014 mg mL^{-1} and a yield of ≈9%. The lateral size of as-produced single- and few-layered MoS_2 nanosheets were as large as 50 μm. By using this exfoliated monolayer MoS_2, the as-made back-gate FET exhibited high on/off ratio

of ≈10^6 and field-effect mobility of 1.2 cm^2 V^{-1} s^{-1}, which were comparable to micromechanically exfoliated nanosheets.

Moreover, sulfonate salts exhibited promising applications on intercalation and subsequent exfoliation of graphite. Wang et al. selected poly(sodium-4-styrenesulfonate) (PSS) as an effective electrolyte to produce graphene sheets under a constant voltage of 5 V for 20 min.[120] The method could produce graphene sheets with a yield of 15% containing single or few layers. The graphene dispersion was stable for 6 months without obvious precipitation. During the process, the edge-to-face interaction between graphene surface and aromatic ring of PSS was responsible for the successful exfoliation. Li et al. used SDBS solution as the electrolyte to produce graphene by applying 30 V for 48 h.[121] SDBS served not only as the intercalant to electrochemically exfoliate graphite but also as a surfactant to stabilize graphene nanosheets. Mensing et al. presented a facile electrochemical method to fabricate graphene-metal phthalocyanines (MePc) hybrid by using the electrolyte containing copper phthalocyanine tetrasulfonic acid.[122] After electrolysis for 12 h between two graphite rod-electrodes and subsequent ultrasonication for 1 h, MePc functionalized graphene was obtained. Kuila et al. employed an alkaline solution of 6-amino-4-hydroxy-2-naphthalene-sulfonic acid (ANS) as the electrolyte as well as surface modifier to exfoliate graphite anode.[123] FTIR, XPS and Raman spectra not only confirmed the functionalization of graphene with ANS, but also revealed the presence of defects mainly due to the formation of oxygen-containing functional groups bound onto the graphene surface.

Inspired by Fukushima et al. who reported the modification of carbon nanotube with ILs,[124] Liu and co-workers later performed the electrochemical exfoliation process in an aqueous solution of ILs (1-octyl-3-methyl-imidazolium hexafluorophosphate) with a two-graphite electrode setup.[125] The results revealed that the lateral size of graphene sheets was 700 nm × 500 nm with an average thickness of 1.1 nm. The interaction between ILs and graphene sheets was attributed to the formation of 1-octyl-3-methylimidazolium free radical, which would interact with π electrons of graphene sheets. The ILs-modified graphene sheets could be used as the filler material for the making graphene/polymer composites. For example, the conductivity of polystyrene composites with ≈4 vol% of graphene was enhanced by more than one order of magnitude compared with that of carbon nanotube/polystyrene composites. Lu and co-workers used the water-miscible ionic liquid, i.e., 1-butyl-3-methylimidazolium tetrafluoroborate [BMIm][BF4], as the electrolyte to study the electrochemical exfoliation process.[126] They proposed that water, the major impurity in ILs, played an important role. It would disrupt the internal organization of ILs by forming new hydrogen-bonded networks. The complex interplay of anodic oxidation of water and subsequent anionic intercalation in the ionic liquid resulted in the expansion and exfoliation of graphite into carbon nanoparticles, nanoribbons and graphene sheets. The IL electrolyte with high water content (>10%) would generate water-soluble and oxidized carbon nanomaterials. Otherwise, IL-functionalized carbon nanomaterials would be produced.

In addition, some other anionic species have also been reported to exfoliate graphite anodes. Khanra et al. used alkaline solution of 9-anthracene carboxylate ion (ACA) as the electrolyte for the graphite exfoliation under a constant voltage (≈20 V) for 10 h and ACA could simultaneously functionalize graphene sheets.[127] XPS indicated that graphite oxidation occurred during the electrochemical exfoliation process. It is suggested that ACA ions were surface absorbed on graphite anode by electrostatic interaction and peeled off together with graphene sheets under the electrical potential. Zeng et al. reported in situ electrochemical exfoliation of graphite in phosphate buffer solution (PBS) by using cyclic voltammatry (CV) scanning at anoidic potentials (0–3 V).[128] The intercalation process resulted in the formation of oxygen functionalities, which weakened the interlayer attraction; the oxidation process facilitated the exfoliation of graphite upon the gas evolution.

3.2. Cationic Intercalations

In the anodic intercalation process, the potentials required for the anions to intercalate are ususally greater than the potentials needed for graphite oxidation,[159] thus the generatation of some oxygen-containing functional groups on graphene surface is unavoidable, and this is detrimental to electronic applications. Since the π-electron system is disrupted, even after the reduction, it is hardly possible to restore the electronic structure. Therefore the cathodic production of graphene was attempted via the intercalation of cations into graphite layers.

Zhou et al. prepared few layered graphene by electrochemical exfoliation of a graphite cathode under a DC voltage of 5 V using Na^+/DMSO complexes as the intercalant. Upon the sonication, graphene dispersions were obtained and graphene sheets showed a lower content of defects and oxygen functional groups.[129] Yang et al. reported the cathodic exfoliation of graphite in ILs *N*-butyl, methylpyrrolidinium bis(trifluoromethylsulfonyl)-imide ($BMPTF_2N$). $[BMP]^+$ cations were intercalated to facilitate the graphite exfoliation.[130]

Li^+ is also a good choice for the intercalation of graphite. As discussed in Section 2.5.1, direct Li-assisted exfoliation requires a high reaction temperature (e.g., 100 °C) and a long reaction time up to several days, and also lacks the controllability of the Li intercalation. Incomplete Li insertion produces a low yield of single-layered 2D materials whereas overinsertion can result in decomposition and the formation of metal nanoparticles and LiS_2.[131] To address these issues, Zeng et al. developed a simple and effective method to fabricate single-layered 2D nanomaterials with high yield through a controllable lithiation process. In this method, bulk layered material, such as MoS_2, WS_2, TiS_2, TaS_2, ZrS_2 and graphite, were incorporated into an electrochemical setup as cathode, and the Li foil served as anode to provide Li ions (**Figure 10**).[132] The reaction mechanism is similar to the direct Li-assisted exfoliation, including the Li^+ intercalation followed by sonication in deionized water. But the efficiency of Li^+ intercalation was remarkably improved under the electrochemical bias,

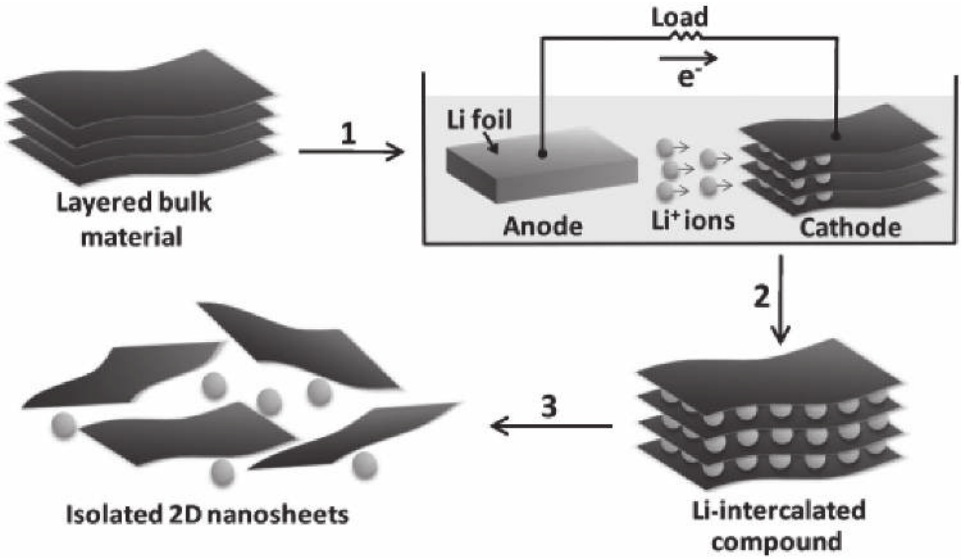

Figure 10. Schematic of electrochemical lithiation process for the production of 2D nanosheets from bulk layered crystals. Reproduced with permission.[132] Copyright 2011, Wiley-VCH.

compared to the previous pure ionic diffusion. This whole process was easily finished within 6 h at room temperature and the lithiation could be monitored and well controlled in a battery system. Characterizations including XPS, TEM, AFM and Raman confirmed the production of single-layered 2D materials with excellent quality and high yield up to 92%. As a proof-of-concept application, FET devices based on single-layered MoS_2 showed p-type semiconducting properties, and thin film transistors based on MoS_2 thin films were used for NO detection.[133] Besides sensing applications,[134–136] other exfoliated 2D TMD nanosheets were used for making composite materials, which showed various promising applications.[137–140] It is worth noting that this method altered the electronic properties from semiconducting to metallic (e.g., MoS_2) and additional annealing at 300 °C was required to restore their intrinsic properties.[21]

Later, Zhang's group further optimized the lithiation process to produce other few-layer-thick inorganic sheets such as h-BN, $NbSe_2$, WSe_2, Sb_2Se_3 and Bi_2Te_3.[141] Unlike the previously reported materials, h-BN and metal selenides or tellurides showed continuously descending discharge curves without a plateau, which rendered it difficult to determine the cut-off voltage for good control of the Li^+ insertion amount. Through the systematic examination of nanomaterials obtained at various cut-off voltages, the electrochemical lithiation process for the fabrication of few-layered nanosheets was successfully optimized. The thermoelectric properties of $NbSe_2$ sheet films were also studied, exhibiting p-type semiconductivity and an enhanced Seebeck coefficient.

Inspired by the electrochemical reactions of negative graphite electrodes in liquid rechargeable Li-ion batteries, Wang and co-workers demonstrated successful exfoliation of graphite in few-layered graphene sheets (<5 layers) with high yield (>70%), in which the negative graphite electrode was electrochemically charged and expanded in an electrolyte of Li salts and propylene carbonate (PC).[142] Li^+/PC complexes were intercalated into graphite interlayers under high current density and graphite was exfoliated via power sonication in concentrated LiCl (dissolved in mixed solvents of DMF/PC). The graphene sheets were dispersed in solvents (e.g., DCB) to form a conducting carbon ink that was brush painted on the commercial papers. As-made graphene paper exhibited a low sheet resistance of 15 Ω sq^{-1}, which was better than that of reduced GO paper.[143]

4. Shear Exfoliation

The sections above have discussed in detail the exfoliation of bulk layered materials with the aid of ultrasonication. Generally, LBE achieved by ultrasonicating bulk layered powders in appropriate liquids (i.e., solvents, and aqueous solutions of surfactants or polymers) can give dispersions of defect-free nanosheets at concentrations of up to ≈1 mg mL^{-1}. However, ultrasonication shows one major drawback in scalability. The production rate of 2D nanomaterials can be given by $P_R = CV/t$, where t is the production time, V is the liquid volume and C is the solution concentration. Because C scales roughly inversely with liquid volume,[144] P_R cannot be scaled up by simply increasing liquid volume. This dramatically limits the utility of ultrasonication as a scalable technique.

Shear mixing has been popular for dispersing aggregated nanoparticles that are weakly bound together in liquids. This method has been reported in papers and patents as part of the process for the exfoliation of graphite and other layered materials.[145–147] In all cases, these bulk layered materials (e.g., graphite and TaS_2) were firstly treated with sulfuric acid, through which intercalated intermediate products with weakened interlayer bonding could be formed, and then the shear force exfoliation was conducted. The synthesized flakes were usually thick, ranging from 10 nm to 100 nm. It is the intercalation process rather than shear force exfoliation that determines the exfoliation efficiency. This also restricts the potential of scaleup production.

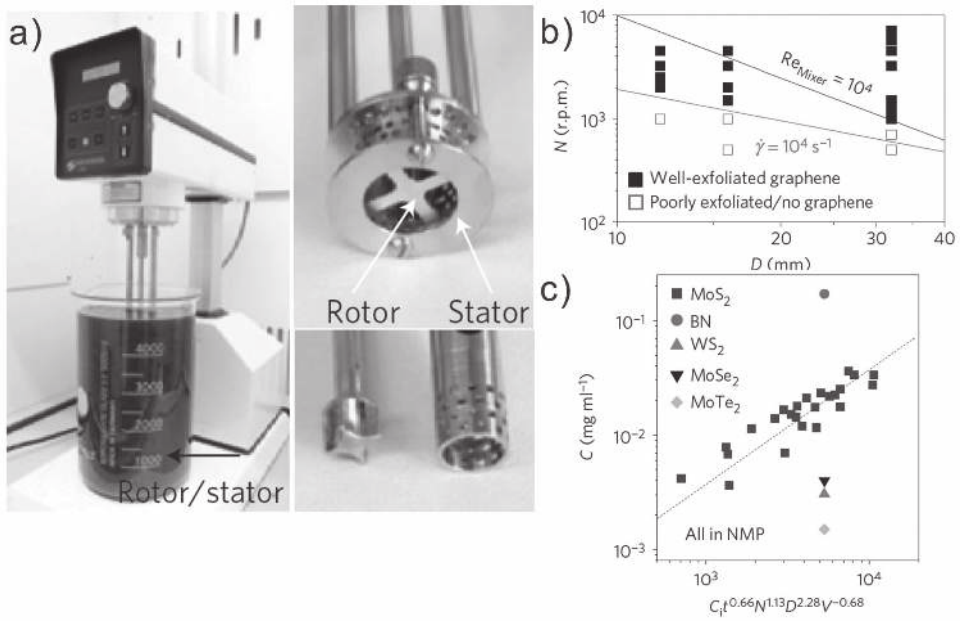

Figure 11. a) Set-up of high shear mixer in graphene dispersion with close-up view of rotor and stator. b) Diagram of rotor speed, N versus diameter, D. The red line represents a minimum shear rate $\gamma \approx 10^4\ s^{-1}$. c) Concentration of 2D nanosheets dispersed in NMP following the certain scaling behavior. Reproduced with permission.[144] Copyright 2014, Nature Publishing Group.

This issue was recently addressed by Coleman's group using a high-shear method without the need for the pre-intercalation step. Paton et al. demonstrated that high-shear mixing of graphite in suitable stabilizing liquids led to large-scale production of defect-free graphene sheets (**Figure 11**a).[144] In this method, the shear mixer consisting of rotor and stator (or rotating blades) was used to generate high shear rates in liquids, to which the layered powders were added. So long as the interaction between liquid media and layered material energetically allows the exfoliation and the liquid can stabilize as-produced nanosheets, the shear forces will cause delamination of nanosheets from the layered crystal. The exfoliation process occured once the local shear rate exceeded $10^4\ s^{-1}$ as unveiled in the simple model (Figure 11b). The scalability of this shear exfoliation method was also carefully investigated, showing that it was closely related to such variables as the initial graphite concentration (C_i), mixing time (t), rotor diameter (D), liquid volume (V) and rotor speed (N). These parameters followed a certain scaling law (Figure 11c). The superlinear relationship between the production rate and the liquid volume made scaleup a reality. The exfoliation could be achieved in liquid volumes up to hundreds of liters with a production rate of 1.44 g h^{-1} for graphene, far higher than previously reported ultrasonication methods. Meanwhile, it gave defect-free nanosheets with dimensions similar to those produced by ultrasonication methods.

As-produced graphene sheets were integrated into a range of different applications, which required a large quantity of good quality graphene nanosheets. For the reinforcement application in polyethylene terephthalate (PET), even low loading levels could result in a 40% increase in strength and a 13% increase in modulus. Graphene thin films showed a high conductivity of 400 S cm^{-1}, and coule therefore be used as electrodes for dye-sensitized solar cells and micro-supercapacitors. Moreover, an elastomer/graphene composite strain sensor was also demonstrated. Importantly, this method is also applicable to other bulk layered materials such as h-BN, MoS_2, WS_2, $MoSe_2$ and $MoTe_2$.

One problem that is specific to shear exfoliation is that rotor/stator mixers tend to give nanosheet concentrations at relatively low levels (<0.1 mg mL^{-1}), limiting the efficiency of the process. While the concentration can be increased to ≈1 mg mL^{-1} using kitchen blenders to obtain 2D nanosheets, such as graphene, MoS_2 etc., the scalability of this technology is not clear.[148,149] Varrla et al. demonstrated the large-scale shear exfoliation of bulk layered materials (e.g., MoS_2, BN and WS_2) in aqueous surfactant solution using a kitchen blender.[148] By optimizing the mixing parameters including nanosheets concentration, liquid volume, rotor speed and mixing time, the production rate could approach on the order of mg min^{-1} scale. The mean nanosheets dimensions are in the range of 40–200 nm for length and 2–12 layers for thickness. Overall, shear exfoliation is a very promising technique, which has already been commercialized as a graphene production technique.

5. Conclusion and Perspectives

In this review article, we have highlighted a variety of methods using LBE to produce 2D nanomaterials. Like any processing method, LBE has many advantages, which must be carefully balanced against its disadvantages. Among its advantages, LBE is clearly a scalable and versatile technique, which has the potential to produce nanosheets extremely cheaply. It is extremely simple to transform layered powder, or even mineral ore[160] to large quantities of nanosheets in

several steps (with or without intercalation, sonication/shear, and centrifugation). This process gives reasonable concentrations up to ≈1 mg mL^{-1}, although higher concentrations can be achieved by solvent removal and redispersion. The process is scalable; using shear exfoliation can give industrial scale volumes and nanosheet production rates. Importantly, the resultant nanosheets tend to be defect-free – the effect of the inputted energy is almost exclusive to exfoliate and cut the nanosheets (i.e., create edges) rather than to create point defects. One of its great strengths is that it can be applied to a host of materials. In addition to graphene, LBE has been used to successfully exfoliate h-BN, transition metal dichalcogenides such as MoS_2, layered metal oxides including MoO_3,[59] the III-VI layered semiconductor GaS,[161] as well as black phosphorous,[53–55] and functionalized layered double hydroxides. Beyond these, there are still a lot of layered materials, which may offer exciting properties, but have not been exfoliated yet. The diversity of exfoliated materials and versatile properties are anticipated for a wide range of applications in electronics, energy storage, bio-sensing, and composites, to name but a few. Another example of its versatility is the range of dispersants which can be used. Most layered materials can be exfoliated using solvents (energy minimization), ionic liquids, surfactants (electrostatic stabilization) and polymers (steric stabilization). This means nanosheets can be obtained in aqueous conditions or a wide range of organic solvents. The resultant wide range of solvent systems helps to make nanosheet dispersions extremely processable. Nanosheet dispersions can be formed into networks or films by a range of processes including inkjet printing.[13,162–168] or spray coating[169] Composite formation is particularly simple, just by removing the solvent from polymer exfoliated nanosheet dispersions[170] or by adding dried exfoliated powder to a melt polymer.[171]

It must be pointed out however, that LBE has a number of significant disadvantages. Most importantly, as-produced nanosheets tend to have broad thickness and lateral size distributions.[172] They tend to have up to 10 layers with low monolayer contents, typically no more than 10% by number (apart from the Li^+ based electrochemical exfoliation which can give monolayer content up to ≈92%). In addition, the size distribution can span from <50 nm[172] to many μm,[173] depending on the material. These problems can be mitigated somewhat by techniques to select nanosheets according to their dimensions. For example, size selection can give dispersions with monolayer contents high enough to be luminescent,[172] or sizes large enough to be effective fillers in composites.[170,171,174] However, a significant problem is that nanosheet thickness and size appear to be correlated with liquid-based exfoliation dispersions such that thinner nanosheets tend to be smaller.[59,172] This significant problem makes it extremely hard to produce large, yet thin nanosheets. Another important problem is the low yield associated with LBE. Exfoliation only converts a very small fraction of layered powder to dispersed nanosheets. While this can be mitigated somewhat by recycling the unconverted material, it does result in a relatively inefficient process. Other, more minor problems are associated with reaggregation of nanosheets on deposition and during film formation and the difficulty in completely removing dispersants such as solvent, surfactant or polymer molecules.

On balance, the strengths and weaknesses of LBE are relatively clear and mean that this method is appropriate for certain applications but not others. For example if defect-free, few-layered nanosheets are appropriate, and easy access to large volumes is a priority, LBE is probably the best option. However, if highly uniform, single-layered or few-layered electronic grade 2D nanomaterials are needed, other methods would be preferable, such as CVD methods.[175]

Acknowledgements

Z. J. Zheng and L. Y. Niu acknowledge GRF of Hong Kong (PolyU 153041/14P; PolyU 5030/12P), The Hong Kong Polytechnic University (A-SA78), and the Innovation and Technology Fund of Hong Kong (ITS/380/14; ITP/067/14TP). J. N. C. acknowledges financial support from Science Foundation Ireland and the European Research Council. H. Z. acknowledges financial support from MOE under AcRF Tier 2 (ARC 26/13, No. MOE2013-T2–1–034; ARC 19/15, No. MOE2014-T2–2–093), AcRF Tier 1 (RGT18/13, RG5/13), NTU under Start-Up Grant (M4081296.070.500000), iFood Research Grant (M4081458.070.5000000), and the Singapore Millennium Foundation in Singapore. H. S. S. acknowledges a NRF grant (No. NRF-2014R1A2A2A01007136) and a grant (Code No. 2011–0031630) from the Center for Advanced Soft Electronics under the Global Frontier Research Program through the National Research Foundation funded by the Ministry of Science, ICT and Future Planning, Korea. M. C. acknowledges the National Science Foundation Division of Graduate Education (NSF DGE) 0903661.

[1] V. Nicolosi, M. Chhowalla, M. G. Kanatzidis, M. S. Strano, J. N. Coleman, *Science* **2013**, *340*, 1420.
[2] C. C. Coleman, H. Goldwhite, W. Tikkanen, *Chem. Mater.* **1998**, *10*, 2794.
[3] R. Z. Ma, T. Sasaki, *Adv. Mater.* **2010**, *22*, 5082.
[4] M. Naguib, M. Kurtoglu, V. Presser, J. Lu, J. J. Niu, M. Heon, L. Hultman, Y. Gogotsi, M. W. Barsoum, *Adv. Mater.* **2011**, *23*, 4248.
[5] X. H. Cao, Z. Y. Yin, H. Zhang, *Energy Environ. Sci.* **2014**, *7*, 1850.
[6] X. Huang, Z. Y. Zeng, Z. X. Fan, J. Q. Liu, H. Zhang, *Adv. Mater.* **2012**, *24*, 5979.
[7] X. Huang, C. L. Tan, Z. Y. Yin, H. Zhang, *Adv. Mater.* **2014**, *26*, 2185.
[8] Z. Y. Yin, J. X. Zhu, Q. Y. He, X. H. Cao, C. L. Tan, H. Y. Chen, Q. Y. Yan, H. Zhang, *Adv. Energy Mater.* **2014**, *4*, 1300574.
[9] X. Huang, Z. Y. Zeng, H. Zhang, *Chem. Soc. Rev.* **2013**, *42*, 1934.
[10] A. K. Geim, K. S. Novoselov, *Nat. Mater.* **2007**, *6*, 183.
[11] X. Huang, Z. Y. Yin, S. X. Wu, X. Y. Qi, Q. Y. He, Q. C. Zhang, Q. Y. Yan, F. Boey, H. Zhang, *Small* **2011**, *7*, 1876.
[12] Y. W. Zhu, S. Murali, W. W. Cai, X. S. Li, J. W. Suk, J. R. Potts, R. S. Ruoff, *Adv. Mater.* **2010**, *22*, 3906.
[13] K. S. Novoselov, V. I. Fal'ko, L. Colombo, P. R. Gellert, M. G. Schwab, K. Kim, *Nature* **2012**, *490*, 192.

[14] L. Britnell, R. V. Gorbachev, R. Jalil, B. D. Belle, F. Schedin, A. Mishchenko, T. Georgiou, M. I. Katsnelson, L. Eaves, S. V. Morozov, N. M. R. Peres, J. Leist, A. K. Geim, K. S. Novoselov, L. A. Ponomarenko, *Science* **2012**, *335*, 947.
[15] Y. Q. Wu, K. A. Jenkins, A. Valdes-Garcia, D. B. Farmer, Y. Zhu, A. A. Bol, C. Dimitrakopoulos, W. J. Zhu, F. N. Xia, P. Avouris, Y. M. Lin, *Nano Lett.* **2012**, *12*, 3062.
[16] X. L. Li, X. R. Wang, L. Zhang, S. W. Lee, H. J. Dai, *Science* **2008**, *319*, 1229.
[17] M. Y. Han, B. Ozyilmaz, Y. B. Zhang, P. Kim, *Phys. Rev. Lett.* **2007**, *98*, 206805.
[18] R. Balog, B. Jorgensen, L. Nilsson, M. Andersen, E. Rienks, M. Bianchi, M. Fanetti, E. Laegsgaard, A. Baraldi, S. Lizzit, Z. Sljivancanin, F. Besenbacher, B. Hammer, T. G. Pedersen, P. Hofmann, L. Hornekaer, *Nat. Mater.* **2010**, *9*, 315.
[19] J. H. Li, L. Y. Niu, Z. J. Zheng, F. Yan, *Adv. Mater.* **2014**, *26*, 5239.
[20] B. Sensale-Rodriguez, T. Fang, R. S. Yan, M. M. Kelly, D. Jena, L. Liu, H. L. Xing, *Appl. Phys. Lett.* **2011**, *99*, 113104.
[21] Q. H. Wang, K. Kalantar-Zadeh, A. Kis, J. N. Coleman, M. S. Strano, *Nat. Nanotechnol.* **2012**, *7*, 699.
[22] M. Chhowalla, H. S. Shin, G. Eda, L. J. Li, K. P. Loh, H. Zhang, *Nat. Chem.* **2013**, *5*, 263.
[23] C. L. Tan, H. Zhang, *Chem. Soc. Rev.* **2015**, 44, 2713.
[24] I. Jo, M. T. Pettes, J. Kim, K. Watanabe, T. Taniguchi, Z. Yao, L. Shi, *Nano Lett.* **2013**, *13*, 550.
[25] Z. Liu, Y. J. Gong, W. Zhou, L. L. Ma, J. J. Yu, J. C. Idrobo, J. Jung, A. H. MacDonald, R. Vajtai, J. Lou, P. M. Ajayan, *Nat. Commun.* **2013**, *4*, 2541.
[26] S. Stankovich, D. A. Dikin, R. D. Piner, K. A. Kohlhaas, A. Kleinhammes, Y. Jia, Y. Wu, S. T. Nguyen, R. S. Ruoff, *Carbon* **2007**, *45*, 1558.
[27] H. A. Becerril, J. Mao, Z. Liu, R. M. Stoltenberg, Z. Bao, Y. Chen, *ACS Nano* **2008**, *2*, 463.
[28] J. N. Coleman, *Acc. Chem. Res.* **2013**, *46*, 14.
[29] A. Ciesielski, P. Samori, *Chem. Soc. Rev.* **2014**, *43*, 381.
[30] R. S. Edwards, K. S. Coleman, *Nanoscale* **2013**, *5*, 38.
[31] H. Liu, Y. C. Du, Y. X. Deng, P. D. Ye, *Chem. Soc. Rev.* **2015**, *44*, 2732.
[32] D. D. L. Chung, *J. Mater. Sci.* **2016**, 51, 554.
[33] Y. Hernandez, V. Nicolosi, M. Lotya, F. M. Blighe, Z. Y. Sun, S. De, I. T. McGovern, B. Holland, M. Byrne, Y. K. Gun'ko, J. J. Boland, P. Niraj, G. Duesberg, S. Krishnamurthy, R. Goodhue, J. Hutchison, V. Scardaci, A. C. Ferrari, J. N. Coleman, *Nat. Nanotechnol.* **2008**, *3*, 563.
[34] C. E. Hamilton, J. R. Lomeda, Z. Z. Sun, J. M. Tour, A. R. Barron, *Nano Lett.* **2009**, *9*, 3460.
[35] A. B. Bourlinos, V. Georgakilas, R. Zboril, T. A. Steriotis, A. K. Stubos, *Small* **2009**, *5*, 1841.
[36] U. Khan, A. O'Neill, M. Lotya, S. De, J. N. Coleman, *Small* **2010**, *6*, 864.
[37] U. Khan, H. Porwal, A. O'Neill, K. Nawaz, P. May, J. N. Coleman, *Langmuir* **2011**, *27*, 9077.
[38] U. Khan, P. May, A. O'Neill, J. N. Coleman, *Carbon* **2010**, *48*, 4035.
[39] A. O'neill, U. Khan, P. N. Nirmalraj, J. Boland, J. N. Coleman, *J. Phys. Chem. C* **2011**, *115*, 5422.
[40] E. Y. Choi, W. S. Choi, Y. B. Lee, Y. Y. Noh, *Nanotechnology* **2011**, *22*, 365601.
[41] W. Qian, R. Hao, Y. L. Hou, Y. Tian, C. M. Shen, H. J. Gao, X. L. Liang, *Nano Res.* **2009**, *2*, 706.
[42] X. Y. Zhang, A. C. Coleman, N. Katsonis, W. R. Browne, B. J. van Wees, B. L. Feringa, *Chem. Commun.* **2010**, *46*, 7539.
[43] J. N. Coleman, M. Lotya, A. O'Neill, S. D. Bergin, P. J. King, U. Khan, K. Young, A. Gaucher, S. De, R. J. Smith, I. V. Shvets, S. K. Arora, G. Stanton, H. Y. Kim, K. Lee, G. Kim, G. S. Duesberg, T. Hallam, J. J. Boland, J. J. Wang, J. F. Donegan, J. C. Grunlan, G. Moriarty, A. Shmeliov, R. J. Nicholls, J. M. Perkins, E. M. Grieveson, K. Theuwissen, D. W. McComb, P. D. Nellist, V. Nicolosi, *Science* **2011**, *331*, 568.
[44] G. Cunningham, M. Lotya, C. S. Cucinotta, S. Sanvito, S. D. Bergin, R. Menzel, M. S. P. Shaffer, J. N. Coleman, *ACS Nano* **2012**, *6*, 3468.
[45] A. O'Neill, U. Khan, J. N. Coleman, *Chem. Mater.* **2012**, *24*, 2414.
[46] U. Khan, A. O'Neill, H. Porwal, P. May, K. Nawaz, J. N. Coleman, *Carbon* **2012**, *50*, 470.
[47] J. M. Yun, Y. J. Noh, C. H. Lee, S. I. Na, S. Lee, S. M. Jo, H. I. Joh, D. Y. Kim, *Small* **2014**, *10*, 2319.
[48] L. Dong, S. Lin, L. Yang, J. J. Zhang, C. Yang, D. Yang, H. B. Lu, *Chem. Commun.* **2014**, *50*, 15936.
[49] L. K. Li, Y. J. Yu, G. J. Ye, Q. Q. Ge, X. D. Ou, H. Wu, D. L. Feng, X. H. Chen, Y. B. Zhang, *Nat. Nanotechnol.* **2014**, *9*, 372.
[50] H. Liu, A. T. Neal, Z. Zhu, Z. Luo, X. F. Xu, D. Tomanek, P. D. D. Ye, *ACS Nano* **2014**, *8*, 4033.
[51] F. N. Xia, H. Wang, Y. C. Jia, *Nat. Commun.* **2014**, *5*, 4458.
[52] W. N. Zhu, M. N. Yogeesh, S. X. Yang, S. H. Aldave, J. S. Kim, S. Sonde, L. Tao, N. S. Lu, D. Akinwande, *Nano Lett.* **2015**, *15*, 1883.
[53] J. R. Brent, N. Savjani, E. A. Lewis, S. J. Haigh, D. J. Lewis, P. O'Brien, *Chem. Commun.* **2014**, *50*, 13338.
[54] J. Kang, J. D. Wood, S. A. Wells, J. H. Lee, X. L. Liu, K. S. Chen, M. C. Hersam, *ACS Nano* **2015**, *9*, 3596.
[55] P. Yasaei, B. Kumar, T. Foroozan, C. H. Wang, M. Asadi, D. Tuschel, J. E. Indacochea, R. F. Klie, A. Salehi-Khojin, *Adv. Mater.* **2015**, *27*, 1887.
[56] A. Castellanos-Gomez, L. Vicarelli, E. Prada, J. O. Island, K. L. Narasimha-Acharya, S. I. Blanter, D. J. Groenendijk, M. Buscema, G. A. Steele, J. V. Alvarez, H. W. Zandbergen, J. J. Palacios, H. S. J. van der Zant, *2D Mater.* **2014**, 1, 025001.
[57] J. D. Wood, S. A. Wells, D. Jariwala, K. S. Chen, E. Cho, V. K. Sangwan, X. L. Liu, L. J. Lauhon, T. J. Marks, M. C. Hersam, *Nano Lett.* **2014**, *14*, 6964.
[58] D. Hanlon, C. Backes, E. Doherty, C. S. Cucinotta, N. C. Berner, C. Boland, K. Lee, P. Lynch, Z. Gholamvand, A. Harvey, S. Zhang, K. Wang, G. Moynihan, A. Pokle, Q. M. Ramasse, N. McEvoy, W. J. Blau, J. Wang, S. Sanvito, D. D. ORegan, G. S. Duesberg, V. Nicolosi, J. N. Coleman, *Nat. Commun.* **2015**, *6*, 8563.
[59] D. Hanlon, C. Backes, T. M. Higgins, M. Hughes, A. O'Neill, P. King, N. McEvoy, G. S. Duesberg, B. M. Sanchez, H. Pettersson, V. Nicolosi, J. N. Coleman, *Chem. Mater.* **2014**, *26*, 1751.
[60] M. Lotya, Y. Hernandez, P. J. King, R. J. Smith, V. Nicolosi, L. S. Karlsson, F. M. Blighe, S. De, Z. M. Wang, I. T. McGovern, G. S. Duesberg, J. N. Coleman, *J. Am. Chem. Soc.* **2009**, *131*, 3611.
[61] M. Lotya, P. J. King, U. Khan, S. De, J. N. Coleman, *ACS Nano* **2010**, *4*, 3155.
[62] S. De, P. J. King, M. Lotya, A. O'Neill, E. M. Doherty, Y. Hernandez, G. S. Duesberg, J. N. Coleman, *Small* **2010**, *6*, 458.
[63] A. A. Green, M. C. Hersam, *Nano Lett.* **2009**, *9*, 4031.
[64] T. Hasan, F. Torrisi, Z. Sun, D. Popa, V. Nicolosi, G. Privitera, F. Bonaccorso, A. C. Ferrari, *Phys. Status Solidi. B* **2010**, *247*, 2953.
[65] R. Hao, W. Qian, L. H. Zhang, Y. L. Hou, *Chem. Commun.* **2008**, 6576.
[66] R. J. Smith, P. J. King, M. Lotya, C. Wirtz, U. Khan, S. De, A. O'Neill, G. S. Duesberg, J. C. Grunlan, G. Moriarty, J. Chen, J. Z. Wang, A. I. Minett, V. Nicolosi, J. N. Coleman, *Adv. Mater.* **2011**, *23*, 3944.
[67] S. Vadukumpully, J. Paul, S. Valiyaveettil, *Carbon* **2009**, *47*, 3288.
[68] S. M. Notley, *Langmuir* **2012**, *28*, 14110.
[69] L. Guardia, M. J. Fernandez-Merino, J. I. Paredes, P. Solis-Fernandez, S. Villar-Rodil, A. Martinez-Alonso, J. M. D. Tascon, *Carbon* **2011**, *49*, 1653.

[70] J. Geng, B. S. Kong, S. B. Yang, H. T. Jung, *Chem. Commun.* **2010**, *46*, 5091.
[71] R. J. Smith, M. Lotya, J. N. Coleman, *New J. Phys.* **2010**, *12, 125008*.
[72] A. B. Bourlinos, V. Georgakilas, R. Zboril, T. A. Steriotis, A. K. Stubos, C. Trapalis, *Solid State Commun.* **2009**, *149*, 2172.
[73] Y. T. Liang, M. C. Hersam, *J. Am. Chem. Soc.* **2010**, *132*, 17661.
[74] P. May, U. Khan, J. M. Hughes, J. N. Coleman, *J. Phys. Chem. C* **2012**, *116*, 24390.
[75] L. X. Xu, J. W. McGraw, F. Gao, M. Grundy, Z. B. Ye, Z. Y. Gu, J. L. Shepherd, *J. Phys. Chem. C* **2013**, *117*, 10730.
[76] T. Skaltsas, N. Karousis, H. J. Yan, C. R. Wang, S. Pispas, N. Tagmatarchis, *J. Mater. Chem.* **2012**, *22*, 21507.
[77] F. Liu, J. Y. Choi, T. S. Seo, *Chem. Commun.* **2010**, *46*, 2844.
[78] M. Zhang, R. R. Parajuli, D. Mastrogiovanni, B. Dai, P. Lo, W. Cheung, R. Brukh, P. L. Chiu, T. Zhou, Z. F. Liu, E. Garfunkel, H. X. He, *Small* **2010**, *6*, 1100.
[79] D. W. Lee, T. Kim, M. Lee, *Chem. Commun.* **2011**, *47*, 8259.
[80] D. Parviz, S. Das, H. S. T. Ahmed, F. Irin, S. Bhattacharia, M. J. Green, *ACS Nano* **2012**, *6*, 8857.
[81] A. Schlierf, H. F. Yang, E. Gebremedhn, E. Treossi, L. Ortolani, L. P. Chen, A. Minoia, V. Morandi, P. Samori, C. Casiraghi, D. Beljonne, V. Palermo, *Nanoscale* **2013**, *5*, 4205.
[82] H. Yang, Y. Hernandez, A. Schlierf, A. Felten, A. Eckmann, S. Johal, P. Louette, J. J. Pireaux, X. Feng, K. Muellen, V. Palermo, C. Casiraghi, *Carbon* **2013**, *53*, 357.
[83] J. H. Jang, D. Rangappa, Y. U. Kwon, I. Honma, *J. Mater. Chem.* **2011**, *21*, 3462.
[84] X. C. Dong, Y. M. Shi, Y. Zhao, D. M. Chen, J. Ye, Y. G. Yao, F. Gao, Z. H. Ni, T. Yu, Z. X. Shen, Y. X. Huang, P. Chen, L. J. Li, *Phys. Rev. Lett.* **2009**, 102, 135501.
[85] X. Q. Wang, P. F. Fulvio, G. A. Baker, G. M. Veith, R. R. Unocic, S. M. Mahurin, M. F. Chi, S. Dai, *Chem. Commun.* **2010**, *46*, 4487.
[86] D. Nuvoli, L. Valentini, V. Alzari, S. Scognamillo, S. B. Bon, M. Piccinini, J. Illescas, A. Mariani, *J. Mater. Chem.* **2011**, *21*, 3428.
[87] L. Y. Niu, M. J. Li, X. M. Tao, Z. Xie, X. C. Zhou, A. P. A. Raju, R. J. Young, Z. J. Zheng, *Nanoscale* **2013**, *5*, 7202.
[88] L. Y. Niu, K. Li, H. Y. Zhen, Y. S. Chui, W. J. Zhang, F. Yan, Z. J. Zheng, *Small* **2014**, *10*, 4651.
[89] M. B. Dines, *Mater. Res. Bull.* **1975**, *10*, 287.
[90] P. Joensen, R. F. Frindt, S. R. Morrison, *Mater. Res. Bull.* **1986**, *21*, 457.
[91] R. Bissessur, M. G. Kanatzidis, J. L. Schindler, C. R. Kannewurf, *J. Chem. Soc. Chem. Comm.* **1993**, 1582.
[92] B. K. Miremadi, S. R. Morrison, *J. Appl. Phys.* **1988**, *63*, 4970.
[93] T. Hibino, W. Jones, *J. Mater. Chem.* **2001**, *11*, 1321.
[94] H. L. Tsai, J. Heising, J. L. Schindler, C. R. Kannewurf, M. G. Kanatzidis, *Chem. Mater.* **1997**, *9*, 879.
[95] R. A. Gordon, D. Yang, E. D. Crozier, D. T. Jiang, R. F. Frindt, *Phys. Rev. B* **2002**, *65*, 125407.
[96] K. Q. Zhou, Y. Q. Shi, S. H. Jiang, L. Song, Y. Hu, Z. Gui, *Mater. Res. Bull.* **2013**, *48*, 2985.
[97] M. S. Dresselhaus, G. Dresselhaus, *Adv. Phys.* **2002**, *51*, 1.
[98] N. I. Kovtyukhova, Y. X. Wang, A. Berkdemir, R. Cruz-Silva, M. Terrones, V. H. Crespi, T. E. Mallouk, *Nat. Chem.* **2014**, *6*, 957.
[99] M. Naguib, V. N. Mochalin, M. W. Barsoum, Y. Gogotsi, *Adv. Mater.* **2014**, *26*, 992.
[100] O. Mashtalir, M. Naguib, V. N. Mochalin, Y. Dall'Agnese, M. Heon, M. W. Barsoum, Y. Gogotsi, *Nat. Commun.* **2013**, 4, 1716.
[101] M. Naguib, O. Mashtalir, J. Carle, V. Presser, J. Lu, L. Hultman, Y. Gogotsi, M. W. Barsoum, *ACS Nano* **2012**, *6*, 1322.
[102] M. Naguib, J. Come, B. Dyatkin, V. Presser, P. L. Taberna, P. Simon, M. W. Barsoum, Y. Gogotsi, *Electrochem. Commun.* **2012**, *16*, 61.
[103] Q. Tang, Z. Zhou, P. W. Shen, *J. Am. Chem. Soc.* **2012**, *134*, 16909.
[104] M. R. Lukatskaya, O. Mashtalir, C. E. Ren, Y. Dall'Agnese, P. Rozier, P. L. Taberna, M. Naguib, P. Simon, M. W. Barsoum, Y. Gogotsi, *Science* **2013**, *341*, 1502.
[105] Y. Dall'Agnese, M. R. Lukatskaya, K. M. Cook, P. L. Taberna, Y. Gogotsi, P. Simon, *Electrochem. Commun.* **2014**, *48*, 118.
[106] Z. Ling, C. E. Ren, M. Q. Zhao, J. Yang, J. M. Giammarco, J. S. Qiu, M. W. Barsoum, Y. Gogotsi, *Proc. Natl. Acad. Sci. USA* **2014**, *111*, 16676.
[107] X. Wang, S. Kajiyama, H. Iinuma, E. Hosono, S. Oro, I. Moriguchi, M. Okubo, A. Yamada, *Nat. Commun.* **2015**, 6, 6544.
[108] M. Q. Zhao, C. E. Ren, Z. Ling, M. R. Lukatskaya, C. F. Zhang, K. L. Van Aken, M. W. Barsoum, Y. Gogotsi, *Adv. Mater.* **2015**, *27*, 339.
[109] Y. Xie, Y. Dall'Agnese, M. Naguib, Y. Gogotsi, M. W. Barsoum, H. L. L. Zhuang, P. R. C. Kent, *ACS Nano* **2014**, *8*, 9606.
[110] E. Yang, H. Ji, J. Kim, H. Kim, Y. Jung, *Phys. Chem. Chem. Phys.* **2015**, *17*, 5000.
[111] T. Sasaki, M. Watanabe, *J. Am. Chem. Soc.* **1998**, *120*, 4682.
[112] Q. L. Wu, A. Olafsen, O. B. Vistad, J. Roots, P. Norby, *J. Mater. Chem.* **2005**, *15*, 4695.
[113] N. Nhlapo, T. Motumi, E. Landman, S. M. C. Verryn, W. W. Focke, *J. Mater. Sci.* **2008**, *43*, 1033.
[114] R. Z. Ma, Z. P. Liu, L. Li, N. Iyi, T. Sasaki, *J. Mater. Chem.* **2006**, *16*, 3809.
[115] M. Osada, T. Sasaki, *J. Mater. Chem.* **2009**, *19*, 2503.
[116] C. Y. Su, A. Y. Lu, Y. P. Xu, F. R. Chen, A. N. Khlobystov, L. J. Li, *ACS Nano* **2011**, *5*, 2332.
[117] K. Parvez, R. J. Li, S. R. Puniredd, Y. Hernandez, F. Hinkel, S. H. Wang, X. L. Feng, K. Mullen, *ACSNano* **2013**, *7*, 3598.
[118] K. Parvez, Z. S. Wu, R. J. Li, X. J. Liu, R. Graf, X. L. Feng, K. Mullen, *J. Am. Chem. Soc.* **2014**, *136*, 6083.
[119] N. Liu, P. Kim, J. H. Kim, J. H. Ye, S. Kim, C. J. Lee, *ACS Nano* **2014**, *8*, 6902.
[120] G. X. Wang, B. Wang, J. Park, Y. Wang, B. Sun, J. Yao, *Carbon* **2009**, *47*, 3242.
[121] P. Li, S. H. Bae, Q. Y. Zan, N. H. Kim, J. H. Lee, *Adv. Mater. Res.*. **2010**, *123–125*, 743.
[122] J. P. Mensing, T. Kerdcharoen, C. Sriprachuabwong, A. Wisitsoraat, D. Phokharatkul, T. Lomas, A. Tuantranont, *J. Mater. Chem.* **2012**, *22*, 17094.
[123] T. Kuila, P. Khanra, N. H. Kim, S. K. Choi, H. J. Yun, J. H. Lee, *Nanotechnology* **2013**, 24, 365706.
[124] T. Fukushima, A. Kosaka, Y. Ishimura, T. Yamamoto, T. Takigawa, N. Ishii, T. Aida, *Science* **2003**, *300*, 2072.
[125] N. Liu, F. Luo, H. X. Wu, Y. H. Liu, C. Zhang, J. Chen, *Adv. Funct. Mater.* **2008**, *18*, 1518.
[126] J. Lu, J. X. Yang, J. Z. Wang, A. L. Lim, S. Wang, K. P. Loh, *ACS Nano* **2009**, *3*, 2367.
[127] P. Khanra, T. Kuila, S. H. Bae, N. H. Kim, J. H. Lee, *J. Mater. Chem.* **2012**, *22*, 24403.
[128] F. W. Zeng, Z. H. Sun, X. G. Sang, D. Diamond, K. T. Lau, X. X. Liu, D. S. Su, *ChemSusChem* **2011**, *4*, 1587.
[129] M. Zhou, J. Tang, Q. Cheng, G. J. Xu, P. Cui, L. C. Qin, *Chem Phys Lett* **2013**, *572*, 61.
[130] Y. C. Yang, F. Lu, Z. Zhou, W. X. Song, Q. Y. Chen, X. B. Ji, *Electrochim Acta* **2013**, *113*, 9.
[131] X. Rocquefelte, F. Boucher, P. Gressier, G. Ouvrard, P. Blaha, K. Schwarz, *Phys. Rev. B* **2000**, *62*, 2397.
[132] Z. Y. Zeng, Z. Y. Yin, X. Huang, H. Li, Q. Y. He, G. Lu, F. Boey, H. Zhang, *Angew. Chem., Int. Ed.* **2011**, *50*, 11093.
[133] Q. Y. He, Z. Y. Zeng, Z. Y. Yin, H. Li, S. X. Wu, X. Huang, H. Zhang, *Small* **2012**, *8*, 2994.
[134] S. X. Wu, Z. Y. Zeng, Q. Y. He, Z. J. Wang, S. J. Wang, Y. P. Du, Z. Y. Yin, X. P. Sun, W. Chen, H. Zhang, *Small* **2012**, *8*, 2264.
[135] C. F. Zhu, Z. Y. Zeng, H. Li, F. Li, C. H. Fan, H. Zhang, *J. Am. Chem. Soc.* **2013**, *135*, 5998.

[136] Y. Zhang, B. Zheng, C. F. Zhu, X. Zhang, C. L. Tan, H. Li, B. Chen, J. Yang, J. Z. Chen, Y. Huang, L. H. Wang, H. Zhang, *Adv. Mater.* **2015**, *27*, 935.
[137] X. Huang, Z. Y. Zeng, S. Y. Bao, M. F. Wang, X. Y. Qi, Z. X. Fan, H. Zhang, *Nat. Commun.* **2013**, 4, 1444.
[138] X. Hong, J. Q. Liu, B. Zheng, X. Huang, X. Zhang, C. L. Tan, J. Z. Chen, Z. X. Fan, H. Zhang, *Adv. Mater.* **2014**, *26*, 6250.
[139] Z. Y. Yin, X. Zhang, Y. Q. Cai, J. Z. Chen, J. I. Wong, Y. Y. Tay, J. W. Chai, J. M. T. Wu, Z. Y. Zeng, B. Zheng, H. Y. Yang, H. Zhang, *Angew. Chem., Int. Ed.* **2014**, *53*, 12560.
[140] Z. Y. Zeng, C. L. Tan, X. Huang, S. Y. Bao, H. Zhang, *Energy Environ. Sci.* **2014**, *7*, 797.
[141] Z. Y. Zeng, T. Sun, J. X. Zhu, X. Huang, Z. Y. Yin, G. Lu, Z. X. Fan, Q. Y. Yan, H. H. Hng, H. Zhang, *Angew. Chem., Int. Ed.* **2012**, *51*, 9052.
[142] J. Z. Wang, K. K. Manga, Q. L. Bao, K. P. Loh, *J. Am. Chem. Soc.* **2011**, *133*, 8888.
[143] D. A. Dikin, S. Stankovich, E. J. Zimney, R. D. Piner, G. H. B. Dommett, G. Evmenenko, S. T. Nguyen, R. S. Ruoff, *Nature* **2007**, *448*, 457.
[144] K. R. Paton, E. Varrla, C. Backes, R. J. Smith, U. Khan, A. O'Neill, C. Boland, M. Lotya, O. M. Istrate, P. King, T. Higgins, S. Barwich, P. May, P. Puczkarski, I. Ahmed, M. Moebius, H. Pettersson, E. Long, J. Coelho, S. E. O'Brien, E. K. McGuire, B. M. Sanchez, G. S. Duesberg, N. McEvoy, T. J. Pennycook, C. Downing, A. Crossley, V. Nicolosi, J. N. Coleman, *Nat. Mater.* **2014**, *13*, 624.
[145] A. Zhamu, J. Shin, J. Guo, B. Z. Jang, US Patent Appl. No.: 11/787,442 **2012**.
[146] L. R. Bunnell, *US patent App1. No.: 791,864*, **1993**.
[147] D. W. Murphy, G. W. Hull, *J. Chem. Phys.* **1975**, *62*, 973.
[148] E. Varrla, C. Backes, K. R. Paton, A. Harvey, Z. Gholamvand, J. McCauley, J. N. Coleman, *Chem. Mater.* **2015**, *27*, 1129.
[149] E. Varrla, K. R. Paton, C. Backes, A. Harvey, R. J. Smith, J. McCauley, J. N. Coleman, *Nanoscale* **2014**, *6*, 11810.
[150] T. J. Mason, J. Phillip, *Applied Sonochemistry*, Wiley-VCH Verlag, Weinheim, **2002**.
[151] J. N. Israelachvili, Intermolecular and Surface Forces, 3rd Ed., Academic Press, Waltham, Massachusetts **2011**.
[152] P. Blake, P. D. Brimicombe, R. R. Nair, T. J. Booth, D. Jiang, F. Schedin, L. A. Ponomarenko, S. V. Morozov, H. F. Gleeson, E. W. Hill, A. K. Geim, K. S. Novoselov, *Nano Lett.* **2008**, *8*, 1704.
[153] X. H. An, T. J. Simmons, R. Shah, C. Wolfe, K. M. Lewis, M. Washington, S. K. Nayak, S. Talapatra, S. Kar, *Nano Lett.* **2010**, *10*, 4295.
[154] J. M. Englert, J. Rohrl, C. D. Schmidt, R. Graupner, M. Hundhausen, F. Hauke, A. Hirsch, *Adv. Mater.* **2009**, *21*, 4265.
[155] A. Ghosh, K. V. Rao, S. J. George, C. N. R. Rao, *Chem. – Eur. J.* **2010**, *16*, 2700.
[156] X. Zhou, T. Wu, K. Ding, B. Hu, M. Hou, B. Han, *Chem. Commun.* **2010**, *46*, 386.
[157] S. G. Gunasekaran, M. Dharmendirakumar, *High Perform. Polym.* **2014**, *26*, 274.
[158] N. I. Kovtyukhova, Y. X. Wang, R. T. Lv, M. Terrones, V. H. Crespi, T. E. Mallouk, *J. Am. Chem. Soc.* **2013**, *135*, 8372.
[159] A. M. Abdelkader, A. J. Cooper, R. A. W. Dryfe, I. A. Kinloch, *Nanoscale* **2015**, *7*, 6944.
[160] N. Savjani, E. A. Lewis, R. A. D. Pattrick, S. J. Haigh, P. O'Brien, *RSC Adv.* **2014**, *4*, 35609.
[161] A. Harvey, C. Backes, Z. Gholamvand, D. Hanlon, D. McAteer, H. C. Nerl, E. McGuire, A. Seral-Ascaso, Q. M. Ramasse, N. McEvoy, S. Winters, N. C. Berner, D. McCloskey, J. F. Donegan, G. S. Duesberg, V. Nicolosi, J. N. Coleman, *Chem. Mater.* **2015**, *27*, 3483.
[162] J. T. Li, M. M. Naiini, S. Vaziri, M. C. Lemme, M. Ostling, *Adv. Funct. Mater.* **2014**, *24*, 6524.
[163] Y. G. Yao, L. Tolentino, Z. Z. Yang, X. J. Song, W. Zhang, Y. S. Chen, C. P. Wong, *Adv. Funct. Mater.* **2013**, *23*, 3577.
[164] F. Torrisi, T. Hasan, W. P. Wu, Z. P. Sun, A. Lombardo, T. S. Kulmala, G. W. Hsieh, S. J. Jung, F. Bonaccorso, P. J. Paul, D. P. Chu, A. C. Ferrari, *ACS Nano* **2012**, *6*, 2992.
[165] K. Y. Shin, J. Y. Hong, J. Jang, *Adv. Mater.* **2011**, *23*, 2113.
[166] J. T. Li, F. Ye, S. Vaziri, M. Muhammed, M. C. Lemme, M. Ostling, *Adv. Mater.* **2013**, *25*, 3985.
[167] L. Huang, Y. Huang, J. J. Liang, X. J. Wan, Y. S. Chen, *Nano Res.* **2011**, *4*, 675.
[168] D. Kong, L. T. Le, Y. Li, J. L. Zunino, W. Lee, *Langmuir* **2012**, *28*, 13467.
[169] L. J. Cao, S. B. Yang, W. Gao, Z. Liu, Y. J. Gong, L. L. Ma, G. Shi, S. D. Lei, Y. H. Zhang, S. T. Zhang, R. Vajtai, P. M. Ajayan, *Small* **2013**, *9*, 2905.
[170] U. Khan, P. May, A. O'Neill, A. P. Bell, E. Boussac, A. Martin, J. Semple, J. N. Coleman, *Nanoscale* **2013**, *5*, 581.
[171] S. B. Xie, O. M. Istrate, P. May, S. Barwich, A. P. Bell, U. Khana, J. N. Coleman, *Nanoscale* **2015**, *7*, 4443.
[172] C. Backes, R. J. Smith, N. McEvoy, N. C. Berner, D. McCloskey, H. C. Nerl, A. O'Neill, P. J. King, T. Higgins, D. Hanlon, N. Scheuschner, J. Maultzsch, L. Houben, G. S. Duesberg, J. F. Donegan, V. Nicolosi, J. N. Coleman, *Nat. Commun.* **2014**, 5, 4576.
[173] U. Khan, A. O'Neill, H. Porwal, P. May, K. Nawaz, J. N. Coleman, *Carbon* **2012**, *50*, 470.
[174] P. May, U. Khan, A. O'Neill, J. N. Coleman, *J. Mater. Chem.* **2012**, *22*, 1278.
[175] M. Chhowalla, Z. F. Liu, H. Zhang, *Chem. Soc. Rev.* **2015**, *44*, 2584.

Received: July 24, 2015
Revised: September 19, 2015
Published online: December 10, 2015

